Cosmology

V.A. Rubakov – *Institute of Nuclear Research, Moscow, Russia. The Full Member of the Russian Academy of Sciences. Scientific interests include: particle physics, quantum theory, supersymmetry and string theory, cosmology, astrophysics, non perturbative methods, neutrino physics.*

Abstract: We review cosmology from the viewpoint of particle physicist. We emphasize the expected impact of the LHC into the understanding of the major cosmological issues, such as the nature and origin of dark matter and generation of matter-antimatter asymmetry. We give several examples showing the LHC potential: WIMPs as cold dark matter candidates, gravitinos as warm dark matter candidates, and electroweak baryogenesis as a possible mechanism for generating matter-antimatter asymmetry. We also overview the results obtained by astronomical methods and discuss expectations for future, with emphasis on their role in revealing the properties of the present and early Universe.

Cosmology

V.A. Rubakov
Institute for Nuclear Research of the Russian Academy of Sciences,
60th October Anniversary Prospect, 7a, 117312 Moscow, Russia

Abstract

We review cosmology from the viewpoint of particle physicist. We emphasize the expected impact of the LHC into the understanding of the major cosmological issues, such as the nature and origin of dark matter and generation of matter-antimatter asymmetry. We give several examples showing the LHC potential: WIMPs as cold dark matter candidates, gravitinos as warm dark matter candidates, and electroweak baryogenesis as a possible mechanism for generating matter-antimatter asymmetry. We also overview the results obtained by astronomical methods and discuss expectations for future, with emphasis on their role in revealing the properties of the present and early Universe.

1 Introduction

The Universe we know of is full of mysteries. It hosts matter but not anti-matter, and after more than 40 years since it was understood that this fact is actually a problem, we do not have an established theory explaining this asymmetry. The Universe hosts dark matter, and we do not know what dark matter it made of. There is dark energy in the Universe whose nature is even more obscure.

Uncovering the physics behind these mysteries is a challenge for both astronomy and particle physics. In particular, strong impact is expected from the LHC. Optimistically, the LHC experiments may discover dark matter particles and their companions, and establish the mechanism of the generation of the matter-antimatter asymmetry. Otherwise they will rule out some very plausible scenarios; this will also have profound consequences on our understanding of the early Universe. There are also exotic hypotheses on physics beyond the Standard Model, like TeV scale gravity; their support by the LHC will have dramatic effect on early cosmology, which is hard to overestimate.

In part of these lectures we concentrate on examples showing the LHC cosmological potential. Before coming to that, we introduce the basic notions of cosmology that will be useful for our main discussion. We then turn to dark matter, and present the WIMP scenario for cold dark matter, which is currently the most popular one – for good reason. We also consider light gravitino scenario for warm dark matter.

Both are to be probed by the LHC, as they require rather particular new physics in the LHC energy range. We then discuss electroweak baryogenesis – a mechanism for the generation of matter-antimatter asymmetry that may have operated in the early Universe at temperature of order 100 GeV. This mechanism also needs new physics at energies $100 - 300$ GeV, so it will be definitely confirmed or ruled out by the LHC.

In another part of these lectures we consider in more detail the cosmological data that have lead to the current picture of the Universe. We also discuss how this picture may evolve as more data are accumulated. The prospects are fascinating: the new data may give strong arguments in favor of the cosmological inflation, they may reveal the mechanism of the generation of the cosmological perturbations thus giving a clue to the very early Universe, they may shed light on the nature of dark energy, provide cosmological measurement of neutrino masses, etc. We may encounter unexpected discoveries such as the evidence for the generation of dark matter and/or baryon asymmetry *before* the hot stage of the cosmological evolution, which would rule out the currently most popular scenarios, including those outlined in these lectures.

These lectures are meant to be self-contained, but we necessarily omit numerous details, while trying to make clear basic ideas and results. More complete accounts of particle physics aspects of cosmology may be found in the books [1] and reviews [2]. Dark matter, including various hypotheses about its particles, is reviewed in [3]. Electroweak baryogenesis is discussed in detail in reviews [4].

In what follows we use natural units,

$$\hbar = c = 1.$$

We also use Mpc as the unit of length,

$$1 \text{ Mpc} = 3 \cdot 10^6 \text{ light yrs} = 3 \cdot 10^{24} \text{ cm}.$$

To give an idea of length scales in the Universe, the distance of the Sun to the center of our Galaxy is 8 kpc, the distance to the nearest galaxy – Andromeda – is 0.8 Mpc, clusters of galaxies have sizes of a few Mpc, the size of the visible part of the Universe is about 15 Gpc.

2 Basics of cosmology

2.1 Friedmann–Robertson–Walker metric

Two basic facts about the Universe are that it is *homogeneous and isotropic* at large spatial scales, and that it *expands*.

There are three types of homogeneous and isotropic three-dimensional spaces.

These are[1] three-sphere, flat space and three-hyperboloid. Accordingly, one speaks about closed, flat and open Universe; in the latter two cases the spatial size of the Universe is infinite, whereas in the former the Universe is compact.

The homogeneity and isotropy of the Universe mean that its hypersurfaces of constant time are either three-spheres or three-planes or three-hyperboloids. The distances between points may (and in fact, do) depend on time, i.e., the interval has the form

$$ds^2 = dt^2 - a^2(t)d\mathbf{x}^2, \tag{1}$$

where $d\mathbf{x}^2$ is the distance on unit three-sphere/plane/hyperboloid. Metric (1) is usually called Friedmann–Robertson–Walker (FRW) metric, and $a(t)$ is called scale factor. In our Universe $\dot{a} \equiv da/dt > 0$, which means that the distance between points of fixed spatial coordinates $\mathbf{x}$ grows, $dl^2 = a^2(t)d\mathbf{x}^2$. The space stretches out; the Universe expands.

The coordinates $\mathbf{x}$ are often called comoving coordinates. It is straightforward to check that $\mathbf{x} = \text{const}$ is a time-like geodesic, so a galaxy put at a certain $\mathbf{x}$ at zero velocity will stay at the same $\mathbf{x}$. Furthermore, as the Universe expands, non-relativistic objects loose their velocities $\dot{\mathbf{x}}$, i.e., they get frozen in the comoving coordinate frame.

Observational data put strong constraints on the spatial curvature of the Universe. They tell that to a very good approximation our Universe is spatially flat, i.e., our *3-dimensional space* is Euclidean. In what follows $d\mathbf{x}^2$ is simply the line interval in Euclidean 3-dimensional space.

2.2 Redshift

Like the distances between free particles in the expanding Universe, the photon wavelength increases too. We will always label the present values of time-dependent quantities by subscript 0: the present wavelength of a photon is thus denoted by λ_0, the present time is t_0, the present value of the scale factor is $a_0 \equiv a(t_0)$, etc. If a photon was emitted at some moment of time t in the past, and its wavelength at the moment of emission was λ, then we receive today a photon whose physical wavelength is longer,

$$\frac{\lambda_0}{\lambda} = \frac{a_0}{a(t)} \equiv 1 + z.$$

Here we introduced the redshift z. The wavelength at emission λ is fixed by physics of the source, say, it is the wavelength of a photon emitted by an excited hydrogen

[1]Strictly speaking, this statement is valid only locally: in principle, homogeneous and isotropic Universe may have complex global properties. As an example, spatially flat Universe may have topology of three-torus. There is some discussion of such a possibility in literature, and fairly strong limits have been obtained by the analyses of cosmic microwave background radiation [5].

atom. Thus, on the one hand, the redshift z is directly measurable[2], and, on the other hand, it is related to the time of emission, and hence to the distance to the source: the light of a very distant source that we receive today was emitted long ago, so that source has large z.

Let us consider a "nearby" source, for which $z \ll 1$. This corresponds to relatively small $(t_0 - t)$. Expanding $a(t)$, one writes

$$a(t) = a_0 - \dot{a}(t_0)(t_0 - t). \tag{2}$$

To the leading order in z, the difference between the present time and the emission time is equal to the distance to the source r (with the speed of light equal to 1). Let us define the Hubble parameter

$$H(t) = \frac{\dot{a}(t)}{a(t)},$$

and denote its present value by H_0. Then eq. (2) takes the form $a(t) = a_0(1 - H_0 r)$, and we get for the redshift, again to the leading non-trivial order in z,

$$1 + z = \frac{1}{1 - H_0 r} = 1 + H_0 r.$$

In this way we obtain *the Hubble law*,

$$z = H_0 r, \quad z \ll 1. \tag{3}$$

Traditionally, one tends to interpret the expansion of the Universe as runaway of galaxies from each other, and red shift as the Doppler effect. Then at small z one writes $z = v$, where v is the radial velocity of the source with respect to the Earth, so H_0 is traditionally measured in units "velocity per distance". Observational data give [7]

$$H_0 = [70.1 \pm 1.3]\ \frac{\text{km/s}}{\text{Mpc}} = (14 \cdot 10^9\ \text{yrs})^{-1}. \tag{4}$$

Traditionally, the present value of the Hubble parameter is written as

$$H_0 = h \cdot 100\ \frac{\text{km}}{\text{s} \cdot \text{Mpc}}. \tag{5}$$

Thus $h \approx 0.7$. We will use this value in further estimates.

Let us point out that the interpretation of redshift in terms of the Doppler effect is actually not adequate, especially for large enough z. In fact, there is no need in

[2]One identifies a series of emission or absorption lines, thus obtaining λ, and measures their actual wavelength λ_0. These spectroscopic measurements give very accurate values of z even for distant sources.

this interpretation at all: the "radial velocity" enters neither theory nor observations, so this notion may be safely dropped. Physically meaningful quantity is redshift z itself.

A final comment is that H_0^{-1} has dimension of time, or length, as indicated in Eq. (4). Clearly, this quantity sets the cosmological scales of time and distance at the present epoch. Indeed, the lifetime of the Universe t_0 and the size of the visible Universe l_0 up to numerical factors are equal to H_0^{-1}, their numerical values are[3] $t_0 = 13.7 \cdot 10^9$ yrs and[4] $l_0 = 14.5$ Gpc $= 44 \cdot 10^9$ light years.

2.3 Hot Universe

Our Universe is filled with cosmic microwave background (CMB). Cosmic microwave background as observed today consists of photons with excellent black-body spectrum of temperature

$$T_0 = 2.725 \pm 0.001 \text{ K}. \tag{6}$$

The spectrum has been precisely measured by various instruments and does not show any deviation from the Planck spectrum [6].

Thus, the present Universe is "warm". Earlier Universe was warmer; it cooled down because of the expansion. While the CMB photons freely propagate today, it was not so at early stage. When the Universe was hot, the usual matter (electrons and protons with rather small admixture of light nuclei) was in the plasma phase. At that time photons strongly interacted with electrons and protons in the plasma, so all these particles were in thermal equilibrium. As the Universe cooled down, electrons "recombined" with protons into neutral hydrogen atoms, and the Universe became transparent to photons. The temperature scale of recombination is, very crudely speaking, determined by the ionisation energy of hydrogen, which is of order 10 eV. In fact, recombination occurred at lower temperature[5], $T_{rec} \approx 3000$ K. An important point is that recombination process lasted quite a bit less than the Hubble time at that epoch; in many cases one can use an approximation that recombination occurred instantaneously.

Another point is that even though after recombination photons no longer were in thermal equilibrium with anything, the shape of the photon distribution function has

[3]The fact that t_0 is numerically very close to H_0^{-1} is actually a coincidence.

[4]The fact that $l_0 > ct_0$ is due to the expansion of the Universe.

[5]One reason is that the number density of electrons and protons was small compared to the number density of photons, i.e., there was large entropy per electron/proton; thus, recombination at higher temperatures was not thermodynamically favourable because of entropy considerations. Another way to understand this is to note that because of small number of protons and electrons, it requires long time for an electron to find proton to recombine with; during that time hydrogen atoms existing in the medium get disintegrated by photons from the high energy tail of the Planck distribution. The latter process is efficient at temperatures well below 10 eV, hence the "delay" of recombination.

not changed, except for overall redshift. Indeed, the thermal distribution function for *ultra-relativistic* particles, the Planck distribution, depends only on the ratio of frequency to temperature, $f_{Planck}(p,T) = f(\omega_p/T)$, $\omega_p = |p|$. As the Universe expands, the frequency gets redshifted, $\omega_p \to \omega_p/(1+z)$, but the shape of the spectrum remains Planckian, with temperature $T/(1+z)$. Hence, the Planckian form of the observed spectrum is no surprise. Generally speaking, this property does not hold for massive particles.

At even earlier times, the temperature of the Universe was even higher. The earliest time which has been observationally probed to date is the Big Bang Nucleosynthesis epoch; it corresponds to temperature of order 1 MeV and lifetime of the Universe of order 1 s.

To summarize, the effective temperature of photons scales as

$$T(t) \propto a^{-1}(t). \tag{7}$$

This behaviour is characteristic to *ultra-relativistic* free spices (at zero chemical potential) only. The same formula is valid (with qualifications, see below) for ultra-relativistic particles (at zero chemical potential) which are in thermal equilibrium. Thermal equilibrium means adiabatic expansion; during adiabatic expansion, the temperature of ultra-relativistic gas scales as the inverse size of the system, according to usual thermodynamics. The energy density of ultra-relativistic gas scales as $\rho \propto T^4$, and pressure is $p = \rho/3$.

Both for free photons, and for photons in thermal equilibrium, the number density behaves as follows,

$$n_\gamma = \text{const} \cdot T^3 \propto a^{-3},$$

and the energy density is given by the Stephan–Boltzmann law,

$$\rho_\gamma = \frac{\pi^2}{30} \cdot 2 \cdot T^4 \propto a^{-4}, \tag{8}$$

where the factor 2 accounts for two photon polarizations. Present number density of relic photons is

$$n_{\gamma,0} = 410 \ \ \text{cm}^{-3}, \tag{9}$$

and their energy density is

$$\rho_{\gamma,0} = 2.7 \cdot 10^{-10} \ \frac{\text{GeV}}{\text{cm}^3}. \tag{10}$$

An important characteristic of the early Universe is the entropy density. It is given by

$$s = \frac{2\pi^2}{45} g_* T^3, \tag{11}$$

where g_* is the number of degrees of freedom[6] with $m \lesssim T$, that is, the degrees of freedom which are relativistic at temperature T. The point is that the entropy density scales *exactly* as a^{-3} (entropy in comoving volume is constant during adiabatic expansion, $sa^3 = \text{const}$), while temperature scales *approximately* as a^{-1}. The present value of the entropy density (taking into account neutrinos as if they were massless) is

$$s_0 \approx 3000 \text{ cm}^{-3}. \tag{12}$$

Let us now turn to non-relativistic particles: baryons, massive neutrinos, dark matter particles, etc. If they are not destroyed during the evolution of the Universe (that is, they are stable and do not co-annihilate), their number density merely gets diluted,

$$n \propto a^{-3}. \tag{13}$$

This means, in particular, that the baryon-to-photon ratio stays constant,

$$\eta \equiv \frac{n_B}{n_\gamma} = \text{const} \approx 6 \cdot 10^{-10}, \tag{14}$$

while the energy density of non-relativistic particles scales as

$$\rho(t) = m \cdot n(t) \propto a^{-3}(t), \tag{15}$$

in contrast to more rapid fall off (8) characteristic to ultra-relativistic spices.

There exists strong evidence for *dark energy* in the Universe, whose density does not decrease in time as fast as in eqs. (8) or (15). We will discuss dark energy in Section 5.5. It suffices to say here that dark energy density, conventionally denoted by ρ_Λ, is approximately constant in time,

$$\rho_\Lambda \approx \text{const}. \tag{16}$$

If the dark energy density is exactly time-independent, it is the same thing as the cosmological constant, or Λ-term.

2.4 Composition of the present Universe

The basic equation governing the expansion rate of the Universe is the Friedmann equation, which we write for the case of spatially flat Universe,

$$H^2 \equiv \left(\frac{\dot{a}}{a}\right)^2 = \frac{8\pi}{3} G\rho, \tag{17}$$

[6]Fermions contribute with a factor 7/8.

where dot denotes derivative with respect to time t, ρ is the *total* energy density in the Universe and G is Newton's gravity constant. In natural units $G = M_{Pl}^{-2}$, where $M_{Pl} = 1.2 \cdot 10^{19}$ GeV is the Planck mass. Let us introduce the parameter

$$\rho_c = \frac{3}{8\pi G} H_0^2 \approx 5 \cdot 10^{-6} \frac{\text{GeV}}{\text{cm}^3}. \tag{18}$$

According to Eq. (17), the sum of all forms of energy density in the present Universe is equal[7] to ρ_c.

As we will now discuss, the cosmological data correspond to a very weird composition of the Universe.

Before proceeding, let us introduce a notion traditional in the analysis of the composition of the present Universe. For every type of matter i with the present energy density $\rho_{i,0}$, one defines the parameter

$$\Omega_i = \frac{\rho_{i,0}}{\rho_c}.$$

Then eq. (17) tells that $\sum_i \Omega_i = 1$ where the sum runs over all forms of energy. Let us now discuss contributions of different spices to this sum.

We begin with **baryons**. The result (14) gives

$$\rho_{B,0} = m_B \cdot n_{B,0} \approx 2.4 \cdot 10^{-7} \ \ \frac{\text{GeV}}{\text{cm}^3}. \tag{19}$$

Comparing this result with the value of ρ_c given in (18), one finds

$$\Omega_B = 0.045.$$

Thus, baryons constitute rather small fraction of the present energy density in the Universe.

Photons contribute even smaller fraction, as is clear from (10), namely $\Omega_\gamma \approx 5 \cdot 10^{-5}$. From electric neutrality, the number density of **electrons** is about the same as that of baryons, so electrons contribute negligible fraction to the total mass density. The remaining known stable particles are **neutrinos**. Their number density is calculable in Hot Big Bang theory and these calculations are nicely confirmed by Big Bang Nucleosynthesis. The number density of each type of neutrinos is $n_{\nu_i} = 112$ cm^{-3} where ν_i are neutrino mass eigenstates. Direct limit on the mass of electron

[7]This would not be the case if our Universe was not spatially flat: positive spatial curvature of the Universe (the case of 3-sphere) gives negative contribution to right hand side of the Friedmann equation, and hence $\rho_0 > \rho_c$, and the opposite for negative spatial curvature (the case of 3-hyperboloid). This is the reason for calling ρ_c the critical density. According to observations, spatial flatness holds to a very good precision, corresponding to less than 2 per cent deviation of total energy density from ρ_c.

neutrino, $m_{\nu_e} < 2.6$ eV, together with the observations of neutrino oscillations suggest that every type of neutrino has mass smaller than 2.6 eV. The energy density of all types of neutrinos is thus smaller than ρ_c:

$$\rho_{\nu,total} = \sum_\alpha m_{\nu_i} n_{\nu_i} < 3 \cdot 2.6 \text{ eV} \cdot 112 \, \frac{1}{\text{cm}^3} \sim 8 \cdot 10^{-7} \, \frac{\text{GeV}}{\text{cm}^3},$$

which means $\Omega_{\nu,total} < 0.16$. This estimate does not make use of any cosmological data. In fact, as we discuss in Section 5.4, cosmological observations give stronger bound on neutrino masses, which corresponds to [7, 8]

$$\Omega_{\nu,total} \lesssim 0.014. \tag{20}$$

We conclude that most of the energy density in the present Universe is not in the form of known particles; most energy in the present Universe must be in "something unknown". Furthermore, there is strong evidence that this "something unknown" has two components: clustered (dark matter) and uncluttered (dark energy).

Clustered dark matter consists presumably of new stable massive particles. These make clumps of energy density which encounter for most of the mass of galaxies and clusters of galaxies. There are a number of ways of estimating the contribution of non-baryonic dark matter into the total energy density of the Universe (see Refs. [3, 9] for details):

– Composition of the Universe affects the angular anisotropy of cosmic microwave background. Quite accurate measurements of the CMB anisotropy, available today, enable one to estimate the total mass density of dark matter.

– Composition of the Universe, and especially the density of non-baryonic dark matter, is crucial for structure formation of the Universe. Comparison of the results of numerical simulations of structure formation with observational data gives reliable estimate of the mass density of non-baryonic clustered dark matter.

The bottom line is that the non-relativistic component constitutes about 28 per cent of the total present energy density, which means that non-baryonic dark matter has

$$\Omega_{DM} \approx 0.23, \tag{21}$$

the rest is due to baryons.

There is direct evidence that dark matter exists in the largest gravitationally bound objects – clusters of galaxies. There are various methods to determine the gravitating mass of a cluster, and even mass distribution in a cluster, which give consistent results. To name a few:

– One measures velocities of galaxies in galactic clusters, and makes use of the gravitational virial theorem,

$$\text{Kinetic energy of a galaxy} = \frac{1}{2} \, \text{Potential energy}.$$

In this way one obtains the gravitational potential, and thus the distribution of the total mass in a cluster.

– Another measurement of masses of clusters makes use of intracluster gas. Its temperature obtained from X-ray measurements is also related to the gravitational potential.

– Fairly accurate reconstruction of mass distributions in clusters is obtained from the observations of gravitational lensing of background galaxies by clusters.

These methods enable one to measure mass-to-light ratio in clusters of galaxies. Assuming that this ratio applies to all matter in the Universe[8], one arrives at the estimate for the mass density of clumped matter in the present Universe. Remarkably, this estimate coincides with (21).

Finally, dark matter exists also in galaxies. Its distribution is measured by the observations of rotation velocities of distant stars and gas clouds around a galaxy.

Thus, cosmologists are confident that much of the energy density in our Universe consists of new stable particles. We will see that there is good chance for the LHC to produce these particles.

Unclustered dark energy. Non-baryonic clustered dark matter is not the whole story. Making use of the above estimates, one obtains an estimate for the energy density of all particles, $\Omega_\gamma + \Omega_B + \Omega_{\nu,total} + \Omega_{DM} \approx 0.3$. This implies that 70 per cent of the energy density is uncluttered. This component is dark energy.

All this fits nicely to all cosmological observations, but does not fit to the Standard Model of particle physics. It is our hope that the LHC will shed light at least on some of the properties of the Universe.

3 Dark matter

Dark matter is characterized by the mass-to-entropy ratio,

$$\left(\frac{\rho_{DM}}{s}\right)_0 = \frac{\Omega_{DM}\rho_c}{s_0} \approx \frac{0.23 \cdot 5 \cdot 10^{-6}\ \text{GeV} \cdot \text{cm}^{-3}}{3000\ \text{cm}^{-3}} = 4 \cdot 10^{-10}\ \text{GeV}. \qquad (22)$$

This ratio is constant in time since the freeze out of dark matter density: both number density of dark matter particles n_{DM} (and hence their mass density $m_{DM}n_{DM}$) and entropy density dilute exactly as a^{-3}.

Dark matter is crucial for our existence, for the following reason. Density perturbations in baryon-electron-photon plasma before recombination do not grow because of high pressure, which is mostly due to photons; instead, perturbations make sound waves propagating in plasma. Hence, in a Universe without dark matter, density perturbations in baryonic component would start to grow only after baryons decouple from photons, i.e., after recombination. The mechanism of the growth is pretty

[8]This is a strong assumption, since only about 10 per cent of galaxies are in clusters.

simple: an overdense region gravitationally attracts surrounding matter; this matter falls into the overdense region, and the density contrast increases. In the expanding matter dominated Universe this gravitational instability results in the density contrast growing like $(\delta\rho/\rho)(t) \propto a(t)$. Hence, in a Universe without dark matter, the growth factor for baryon density perturbations would be at most[9]

$$\frac{a(t_0)}{a(t_{rec})} = 1 + z_{rec} = \frac{T_{rec}}{T_0} \approx 10^3. \tag{23}$$

The initial amplitude of density perturbations is very well known from the CMB anisotropy measurements, $\delta\rho/\rho = 5 \cdot 10^{-5}$. Hence, a Universe without dark matter would still be pretty homogeneous: the density contrast would be in the range of a few per cent. No structure would have been formed, no galaxies, no life. No structure would be formed in future either, as the accelerated expansion due to dark energy will soon terminate the growth of perturbations.

Since dark matter particles decoupled from plasma much earlier than baryons, perturbations in dark matter started to grow much earlier. The corresponding growth factor is larger than (23), so that the dark matter density contrast at galactic and subgalactic scales becomes of order one, perturbations enter non-linear regime and form dense dark matter clumps at $z = 5 - 10$. Baryons fall into potential wells formed by dark matter, so dark matter and baryon perturbations evolve together soon after recombination. Galaxies get formed in the regions where dark matter was overdense originally. The development of perturbations in our Universe is shown in Fig. 1. For this picture to hold, dark matter particles must be non-relativistic early enough, as relativistic particles pass through gravitational wells instead of being trapped there.

Depending on the mass of the dark matter particles and mechanism of their production in the early Universe, dark matter may be *cold* (CDM) and *warm* (WDM). Roughly speaking, CDM consists of heavy particles, while the masses of WDM particles are smaller,

$$\text{CDM} : \quad m_{DM} \gtrsim 10 \text{ keV}, \tag{24}$$

$$\text{WDM} : \quad m_{DM} = 1 - 10 \text{ keV}. \tag{25}$$

We will discuss warm dark matter option later on, and now we move on to CDM.

3.1 WIMPS: Best guess for cold dark matter

There is a simple mechanism of the dark matter generation in the early Universe. It applies to *cold* dark matter. Because of its simplicity and robustness, it is considered by many as a very likely one, and the corresponding dark matter candidates – weakly

[9]Because of the presence of dark energy, the growth factor is even somewhat smaller.

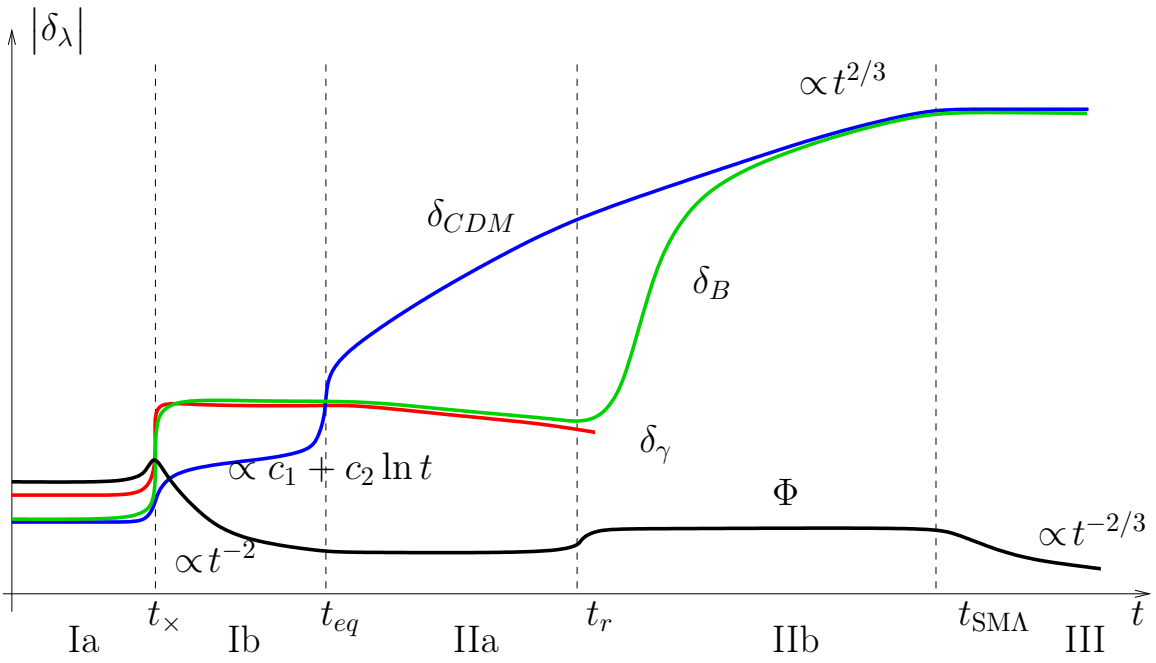

Figure 1: Time dependence, in the linear regime, of density contrasts of dark matter, baryons and photons, $\delta_{DM} \equiv \delta\rho_{DM}/\rho_{DM}$, δ_B and δ_γ, respectively, as well as the Newtonian potential Φ. t_{eq} and t_Λ correspond to the transitions from radiation domination to matter domination, and from decelerated expansion to accelerated expansion.

interacting massive particles, WIMPs – as the best candidates. Let us describe this mechanism in some detail.

Let us assume that there exists a heavy stable neutral particle Y, and that Y-particles can only be destroyed or created via their pair-annihilation or creation, with annihilation products being the particles of the Standard Model. We will see that the overall cosmological behaviour of Y-particles is as follows. At high temperatures, $T \gg m_Y$, the Y-particles are in thermal equilibrium with the rest of cosmic plasma; there are lots of Y-particles in the plasma, which are continuously created and annihilate. As the temperature drops below m_Y, the equilibrium number density decreases. At some "freeze-out" temperature T_f the number density becomes so small, that Y-particles can no longer meet each other during the Hubble time, and their annihilation terminates. After that the number density of survived Y's decreases like a^{-3}, and these relic particles contribute to the mass density in the present Universe. Our purpose is to estimate the range of properties of Y-particles, in which they serve as dark matter.

Assuming thermal equilibrium, elementary considerations of mean free path of a particle in gas give for the lifetime of a non-relativistic Y-particle in cosmic plasma,

τ_{ann},

$$\sigma_{ann} \cdot v \cdot \tau_{ann} \cdot n_Y \sim 1,$$

where v is the velocity of Y-particle, σ_{ann} is the annihilation cross section at velocity v and n_Y is the equilibrium number density given by the Boltzmann law at zero chemical potential[10],

$$n_Y = g_Y \cdot \left(\frac{m_Y T}{2\pi}\right)^{3/2} \mathrm{e}^{-\frac{m_Y}{T}},$$

where g_Y is the number of spin states of Y-particle. Let us assume for definiteness that the annihilation occurs in s-wave (other cases give similar, but not exactly the same results), so at non-relativistic velocities $\sigma_{ann} = \sigma_0/v$, where σ_0 is a constant. One should compare the lifetime with the Hubble time, or annihilation rate $\Gamma_{ann} \equiv \tau_{ann}^{-1}$ with the expansion rate H. At $T \sim m_Y$, the equilibrium density is of order $n_Y \sim T^3$, and $\Gamma_{ann} \gg H$ for not too small σ_0. This means that annihilation (and, by reciprocity, creation) of Y-pairs is indeed rapid, and Y-particles are indeed in thermal equilibrium with the plasma. At very low temperature, on the other hand, the number density n_Y is exponentially small, and $\Gamma_{ann} \ll H$. At low temperatures we cannot, of course, make use of equilibrium formulas: Y-particles no longer annihilate (and, by reciprocity, are no longer created), there is no thermal equilibrium with respect to creation–annihilation processes, and the number density n_Y gets diluted only because of the cosmological expansion.

The freeze-out temperature T_f is determined by the relation

$$\tau_{ann}^{-1}(T_f) \equiv \Gamma_{ann}(T_f) \sim H(T_f),$$

where we can still use the equilibrium formulas, as Y-particles are in thermal equilibrium (with respect to annihilation and creation) just before freeze-out. From Eq. (17) and the Stephan–Boltzmann law one finds that the Hubble parameter at the radiation dominated stage is

$$H = \frac{T^2}{M_{Pl}^*},$$

where $M_{Pl}^* = M_{Pl}/(1.66\sqrt{g_*})$. Making use of this relation we obtain

$$\sigma_0 \cdot n_Y(T_f) \sim \frac{T_f^2}{M_{Pl}^*}, \tag{26}$$

or

$$\sigma_0 \cdot g_Y \cdot \left(\frac{m_Y T_f}{2\pi}\right)^{3/2} \mathrm{e}^{-\frac{m_Y}{T_f}} \sim \frac{T_f^2}{M_{Pl}^*}.$$

[10]The chemical potential is zero, since Y-particles can be pair created, and their number is not conserved.

The latter equation gives the freeze-out temperature, which, up to loglog terms, is

$$T_f \approx \frac{m_Y}{\ln(M_{Pl}^* m_Y \sigma_0)}.$$

Note that this temperature is somewhat smaller than m_Y, if the relevant microscopic mass scale is much below M_{Pl}. This means that Y-particles freeze out when they are indeed non-relativistic, hence the term "cold dark matter". The fact that the annihilation and creation of Y-particles terminates at relatively low temperature has to do with rather slow expansion of the Universe, which should be compensated for by the smallness of the number density n_Y.

At the freeze-out temperature, we make use of eq. (26) and obtain

$$n_Y(T_f) = \frac{T_f^2}{M_{Pl}^* \sigma_0}.$$

Note that this density is inversely proportional to the annihilation cross section (up to logarithms). The reason is that for higher annihilation cross section, the creation–annihilation processes are longer in equilibrium, and less Y-particles survive.

Up to a numerical factor of order 1, the number-to-entropy ratio at freeze-out is

$$\frac{n_Y}{s} \simeq \frac{1}{g_*(T_f) M_{Pl}^* T_f \sigma_0}. \tag{27}$$

This ratio stays constant until the present time, so the present number density of Y-particles is $n_{Y,0} = s_0 \cdot (n_Y/s)_{freeze-out}$, and the mass-to-entropy ratio is

$$\frac{\rho_{Y,0}}{s_0} = \frac{m_Y n_{Y,0}}{s_0} \simeq \frac{\ln(M_{Pl}^* m_Y \sigma_0)}{g_*(T_f) M_{Pl}^* \sigma_0}.$$

This formula is remarkable. The mass density depends mostly on one parameter, the annihilation cross section σ_0. The dependence on the mass of Y-particle is through the logarithm and through $g_*(T_f)$, and is very mild. The value of the logarithm here is between 20 and 40, depending on parameters (this means, in particular, that freeze-out occurs when the temperature drops 20 to 40 times below the mass of Y-particle). Plugging in other numerical values ($g_*(T_f) \sim 100$, $M_{Pl}^* \sim 10^{18}$ GeV), as well as numerical factor omitted in Eq. (27), and comparing with (22) we obtain the estimate

$$\sigma_0 \equiv \langle \sigma v \rangle = (1 \div 2) \cdot 10^{-36} \text{ cm}^2 = (1 \div 2) \text{ pb}. \tag{28}$$

This is weak scale cross section, which tells us what the relevant energy scale is: this is TeV scale. We note in passing that the estimate (28) is rather precise and robust.

The annihilation cross section may be parametrized as $\sigma_0 = \alpha^2/M^2$ where α is some coupling constant, and M is the mass scale (which may be higher than m_Y).

This parametrization is suggested by the picture of Y pair-annihilation via exchange of another particle of mass M. With $\alpha \sim 10^{-2}$, the estimate for the mass scale is roughly $M \sim 1$ TeV. Thus, with very mild assumptions, we find that the non-baryonic dark matter may naturally originate from the TeV-scale physics. In fact, what we have found can be understood as an approximate equality between the cosmological parameter, mass-to-entropy ratio of dark matter, and the particle physics parameters,

$$\text{mass-to-entropy} \simeq \frac{1}{M_{Pl}} \left(\frac{\text{TeV}}{\alpha_W} \right)^2 .$$

Both are of order 10^{-10} GeV, and it is very tempting to think that this is not a mere coincidence. If it is not, the dark matter particle should be found at the LHC.

Of course, the most prominent candidate for WIMP is neutralino of the supersymmetric extension of the Standard Model. The situation with neutralino is somewhat tense, however. The point is that the pair-annihilation of neutralinos often occurs in p-wave, rather than in s-wave. This gives the suppression factor in $\langle \sigma_{ann} v \rangle$, proportional to $v \sim \sqrt{T_f/m_Y} \sim 1/5$. Hence, neutralinos tend to be overproduced in most of the parameter space of MSSM and other models. Yet neutralino remains a good candidate, especially at high $\tan\beta$.

3.2 Warm dark matter: light gravitinos

The cold dark matter scenario successfully describes the bulk of the cosmological data. Yet, there are clouds above it. First, according to numerical simulations, CDM scenario tends to overproduce small objects – dwarf galaxies: it predicts hundreds of satellite dwarf galaxies in the vicinity of a large galaxy like Milky Way whereas about 20 satellites have been observed so far. Second, again according to simulations, CDM tends to produce too high densities in galactic centers (cusps in density profiles); this feature is not confirmed by observations either. There is no crisis yet, but one may be motivated to analyse a possibility that dark matter is not that cold.

An alternative to CDM is warm dark matter whose particles decouple being relativistic. Then their spatial momenta decrease as a^{-1}, i.e., the momenta are of order T all the time after decoupling. WDM particles become non-relativistic at $T \sim m$, where m is their mass. Only after that the WDM perturbations start to grow[11]: as we mentioned above, relativistic particles escape from gravitational potentials, so the gravitational potentials get smeared out instead of getting deeper. Before becoming non-relativistic, WDM particles travel the distance of the order of the horizon size; the WDM perturbations therefore are suppressed at those scales. The horizon size at the time t_{nr} when $T \sim m$ is of order

$$l(t_{nr}) \simeq H^{-1}(T \sim m) = \frac{M^*_{Pl}}{T^2} \sim \frac{M^*_{Pl}}{m^2}.$$

[11] The situation in fact is somewhat more complicated, but this will be irrelevant for our estimates.

Due to the expansion of the Universe, the corresponding length at present is

$$l_0 = l(t_{nr})\frac{a_0}{a(t_{nr})} \sim l(t_{nr})\frac{T}{T_0} \sim \frac{M_{Pl}}{mT_0}, \tag{29}$$

where we neglected (rather weak) dependence on g_*. Hence in WDM scenario, objects of the size smaller than l_0 are less abundant as compared to CDM. Let us point out that l_0 refers to the size of the perturbation as if it were in the linear regime; in other words, this is the size of the region from which matter clumps into a compact object.

The present size of a dwarf galaxy is a few kpc, and the density is about 10^6 of the average density in the Universe. Hence, the size l_0 for these objects is of order 100 kpc $\simeq 3 \cdot 10^{23}$ cm. Requiring that perturbations of this size, but not much larger, are suppressed, we obtain from (29) the estimate (25) for the mass of WDM particles.

To avoid confusion, we point out here that the above reasoning applies to particles whose momenta at decoupling are of order of temperature. While this is the case for many WDM production mechanisms, there exist dark matter production mechanisms that grossly violate this assumption. A famous example is axions whose momenta are always (almost) equal to zero. Despite very small mass of axion, it is a candidate to *cold* dark matter.

Among candidates to WDM particles, light gravitino is probably the best motivated. The gravitino mass is of order

$$m_{3/2} \simeq \frac{F}{M_{Pl}},$$

where $\sqrt{F}$ is the supersymmetry breaking scale. Hence, gravitino masses are in the right ballpark for rather low supersymmetry breaking scales, $\sqrt{F} \sim 10^6 - 10^7$ GeV. This situation can occur, e.g., in gauge mediation scenario. With so low mass, gravitino lifetime is much greater than the age of the Universe, so from this viewpoint gravitinos can indeed serve as dark matter particles. For what follows, important parameters are the widths of decays of other superpartners into gravitino and the Standard Model particles. These are of order

$$\Gamma_{\tilde{S}} \simeq \frac{M_{\tilde{S}}^5}{F^2} \simeq \frac{M_{\tilde{S}}^5}{m_{3/2}^2 M_{Pl}^2}, \tag{30}$$

where $M_{\tilde{S}}$ is the mass of the superpartner.

One mechanism of the gravitino production in the early Universe is decays of other superpartners. Gravitino interacts with everything else so weakly, that once produced, it moves freely, without interacting with cosmic plasma. At production, gravitinos are relativistic, hence they are indeed *warm* dark matter candidates. Let us assume that production in decays is the dominant mechanism and consider under

what circumstances the present mass density of gravitinos coincides with that of dark matter.

The rate of gravitino production in decays of superpartners of the type $\tilde{S}$ in the early Universe is

$$\frac{d(n_{3/2}/s)}{dt} = \frac{n_{\tilde{S}}}{s}\Gamma_{\tilde{S}},$$

where $n_{3/2}$ and $n_{\tilde{S}}$ are number densities of gravitinos and superpartners, respectively, and s is the entropy density. For superpartners in thermal equilibrium, one has $n_{\tilde{S}}/s = \text{const} \sim g_*^{-1}$ for $T \gtrsim M_{\tilde{S}}$, and $n_{\tilde{S}}/s \propto \exp(-M_{\tilde{S}}/T)$ at $T \ll M_{\tilde{S}}$. Hence, the production is most efficient at $T \sim M_{\tilde{S}}$, when the number density of superpartners is still large, while the Universe expands most slowly. The density of gravitinos produced in decays of $\tilde{S}$'s is thus given by

$$\frac{n_{3/2}}{s} \simeq \left(\frac{d(n_{3/2}/s)}{dt}\cdot H^{-1}\right)_{T\sim M_{\tilde{S}}} \simeq \frac{\Gamma_{\tilde{S}}}{g_*}H^{-1}(T\sim M_{\tilde{S}}) \simeq \frac{1}{g_*}\cdot\frac{M_{\tilde{S}}^5}{m_{3/2}^2 M_{Pl}^2}\cdot\frac{M_{Pl}^*}{M_{\tilde{S}}^2}.$$

This gives the mass-to-entropy ratio today:

$$\frac{m_{3/2}n_{3/2}}{s} \simeq \sum_{\tilde{S}} \frac{M_{\tilde{S}}^3}{g_*^{3/2} M_{Pl} m_{3/2}}, \tag{31}$$

where the sum runs over all superpartner spices *which have ever been in thermal equilibrium*. The correct value (22) is obtained for gravitino masses in the range (25) at

$$M_{\tilde{S}} = 100 - 300 \text{ GeV}. \tag{32}$$

Thus, the scenario with gravitino as warm dark matter particle requires light superpartners, which are to be discovered at the LHC.

A few comments are in order. First, decays of superpartners is not the only mechanism of gravitino production: gravitinos may also be produced in scattering of superpartners. To avoid overproduction of gravitinos in the latter processes, one has to assume that the maximum temperature in the Universe (reached after post-inflationary reheating stage) is quite low, $T_{max} \sim 1-10$ TeV. This is not a particularly plausible assumption, but it is consistent with phenomenology and can indeed be realized in some models of inflation. Second, existing constraints on masses of strongly interacting superpartners (squarks and gluinos) suggest that their masses exceed (32). Hence, these particles should not contribute to the sum in (31), otherwise WDM gravitinos would be overproduced. This is possible, if masses of squarks and gluinos are larger than T_{max}, so that they were never abundant in the early Universe. Finally, the decay into gravitino and the Standard Model particles is the only decay channel for the next-to-lightest superpartner (NLSP). Hence, the estimate for the total width of NLSP is given by (30), so that

$$c\tau_{NLSP} = \text{a few} \cdot \text{mm} - \text{a few} \cdot 100 \text{ m}$$

for $m_{2/3} = 1 - 10$ keV and $M_{NLSP} = 100 - 300$ GeV. Thus, NLSP should either be visible in a detector, or fly it through.

Needless to say, the outlined scenario is a lot more contrived than WIMP option. It is reassuring, however, that it can be ruled out or confirmed by the LHC.

3.3 Discussion

If dark matter particles are indeed WIMPs, and the relevant energy scale is of order 1 TeV, then the Hot Big Bang theory will be probed experimentally up to temperature of (a few) $\cdot$ $(10 - 100)$ GeV and down to age $10^{-9} - 10^{-11}$ s in relatively near future (compare to 1 MeV and 1 s accessible today through Big Bang Nucleosynthesis). With microscopic physics to be known from collider experiments, the WIMP density will be reliably calculated and checked against data from observational cosmology. Thus, WIMP scenario offers a window to a very early stage of the evolution of the Universe.

If dark matter particles are gravitinos, the prospect of accessing quantitatively so early stage of the cosmological evolution is not so bright: it would be very hard, if at all possible, to get an experimental handle on the value of the gravitino mass; furthermore, the present gravitino mass density depends on an unknown reheat temperature T_{max}. On the other hand, if this scenario is realized in Nature, then the whole picture of the early Universe will be quite different from what we think today is the most likely early cosmology. Indeed, gravitino scenario requires low reheat temperature, which in turn calls for rather exotic mechanisms of inflation, etc.

The mechanisms discussed here are by no means the only mechanisms capable of producing dark matter, and WIMPs and gravitinos are by no means the only candidates for dark matter particles. Other dark matter candidates include axions, sterile neutrinos, Q-balls, very heavy relics produced towards the end of inflation, etc. Hence, even though there are grounds to hope that the dark matter problem will be solved by the LHC, there is no guarantee at all.

4 Baryon asymmetry of the Universe

In the present Universe, there are baryons and almost no anti-baryons. The number density of baryons today is characterized by the ratio η, see eq. (14). In the early Universe, the appropriate quantity is

$$\Delta_B = \frac{n_B - n_{\overline{B}}}{s},$$

where $n_{\overline{B}}$ is the number density of anti-baryons, and s is the entropy density. If the baryon number is conserved, and the Universe expands adiabatically, Δ_B is constant,

and its value is, up to a numerical factor, equal to η (cf. (9) and (12)), so that

$$\Delta_B \approx 0.8 \cdot 10^{-10}.$$

Back at early times, at temperatures well above 100 MeV, cosmic plasma contained many quark-antiquark pairs, whose number density was of the order of the entropy density,

$$n_q + n_{\bar{q}} \sim s,$$

while baryon number density was related to densities of quarks and antiquarks as follows (baryon number of a quark equals 1/3),

$$n_B = \frac{1}{3}(n_q - n_{\bar{q}}).$$

Hence, in terms of quantities characterizing the very early epoch, the baryon asymmetry may be expressed as

$$\Delta_B \sim \frac{n_q - n_{\bar{q}}}{n_q + n_{\bar{q}}}.$$

We see that there was one extra quark per about 10 billion quark-antiquark pairs! It is this tiny excess that is responsible for entire baryonic matter in the present Universe.

4.1 Sakharov conditions

There is no logical contradiction to suppose that the tiny excess of quarks over antiquarks was built in as an initial condition. This is not at all satisfactory for a physicist, however. Furthermore, inflationary scenario does not provide such an initial condition for Hot Big Bang; rather, inflation theory predicts that the Universe was baryon-symmetric just after inflation. Hence, one would like to explain the baryon asymmetry dynamically.

The baryon asymmetry may be generated from initially symmetric state only if three necessary conditions, dubbed Sakharov's conditions, are satisfied. These are

(i) baryon number non-conservation;

(ii) C- and CP-violation;

(iii) deviation from thermal equilibrium.

All three conditions are easily understood. (i) If baryon number were conserved, and initial net baryon number in the Universe was zero, the Universe today would be symmetric rather than asymmetric. (ii) If C or CP were conserved, then the rates of reactions with particles would be the same as the rates of reactions with antiparticles. In other words, if the initial state of the Universe was C- and CP-symmetric, then the asymmetry between particles and antiparticles may develop only if C and CP is violated. (iii) Thermal equilibrium means that the system is stationary (no time

dependence at all). Hence, if the initial baryon number is zero, it is zero forever, unless there are deviations from thermal equilibrium.

There are two well understood mechanisms of baryon number non-conservation. One of them emerges in Grand Unified Theories and is due to the exchange of supermassive particles. It is very similar, say, to the mechanism of charm non-conservation in weak interactions which occurs via the exchange of heavy W-bosons. The scale of these new, baryon number violating interactions is the Grand Unification scale, presumably of order 10^{16} GeV.

Another mechanism is non-perturbative and is related to the triangle anomaly in the baryonic current (a keyword here is "sphaleron"). It exists already in the Standard Model, and, possibly with slight modifications, operates in all its extensions. The two main features of this mechanism, as applied to the early Universe, is that it is effective over a wide range of temperatures, 100 GeV $< T <$ 10^{11} GeV, and that it conserves $(B - L)$.

4.2 Electroweak baryon number non-conservation

Let us pause here to discuss the physics behind electroweak baryon and lepton number non-conservation in little more detail, though still at a qualitative level. The first thing to consider is the baryonic current,

$$B^\mu = \frac{1}{3} \cdot \sum_i \overline{q}_i \gamma_\mu q_i,$$

where the sum runs over quark flavors. Naively, baryonic current is conserved, but at the quantum level its divergence is not zero, due to the effect called triangle anomaly (axial anomaly in the context of QED and QCD),

$$\partial_\mu B^\mu = \frac{1}{3} \cdot 3_{colors} \cdot 3_{generations} \cdot \frac{g_W^2}{32\pi^2} \epsilon^{\mu\nu\lambda\rho} F^a_{\mu\nu} F^a_{\lambda\rho},$$

where $F^a_{\mu\nu}$ and g_W are the field strength of the $SU(2)_W$ gauge field and the $SU(2)_W$ coupling, respectively. Likewise, each leptonic current ($n = e, \mu, \tau$) is anomalous,

$$\partial_\mu L^\mu_n = \frac{g_W^2}{32\pi^2} \cdot \epsilon^{\mu\nu\lambda\rho} F^a_{\mu\nu} F^a_{\lambda\rho}.$$

A non-trivial fact is that there exist large field fluctuations, $F^a_{\mu\nu}(\mathbf{x}, t) \propto g_W^{-1}$ which have

$$Q \equiv \int d^3x dt \; \frac{g_W^2}{32\pi^2} \cdot \epsilon^{\mu\nu\lambda\rho} F^a_{\mu\nu} F^a_{\lambda\rho} \neq 0.$$

Furthermore, for any such fluctuation the value of Q is integer. Suppose now that a fluctuation with non-vanishing Q has occurred. Then the baryon numbers in the end

and beginning of the process are different,

$$B_{fin} - B_{in} = \int d^3x dt\ \partial_\mu B^\mu = 3Q. \tag{33}$$

Likewise

$$L_{n,\ fin} - L_{n,\ in} = Q. \tag{34}$$

This explains the selection rule mentioned above: B is violated, $(B - L)$ is not.

At zero temperature, the large field fluctuations that induce baryon and lepton number violation are vacuum fluctuations, called instantons, which to a certain extent are similar to virtual fields that emerge and disappear in vacuum of quantum field theory at the perturbative level. The difference is that instantons are *large* field fluctuations. The latter property results in the exponential suppression of the corresponding probability, and hence the rate of baryon number violating processes. In electroweak theory, the suppression factor is extremely small,

$$\mathrm{e}^{-\frac{16\pi^2}{g_W^2}} \sim 10^{-165}.$$

On the other hand, at high temperatures there are large *thermal* fluctuations – "sphalerons" – whose rate is not necessarily small. And, indeed, B-violation in the early Universe is rapid as compared to the cosmological expansion at sufficiently high temperatures, when

$$\langle\phi\rangle_T < T, \tag{35}$$

where $\langle\phi\rangle_T$ is the Higgs expectation value at temperature T.

One may wonder how baryon number may be not conserved even though there are no baryon number violating terms in the Lagrangian of the Standard Model. Let us sketch what is going on (see Ref. [10] for details). Let us consider a massless left handed fermion field in the background of the $SU(2)$ gauge field $\mathbf{A}(\mathbf{x}, t)$, which depends on space-time coordinates in a non-trivial way. As a technical remark, we set the temporal component of the gauge field equal to zero, $A_0 = 0$, by the choice of gauge, and omit the group index. One way to understand the behavior of the fermion field in the gauge field background is to study the system of eigenvalues of the Dirac Hamiltonian $\{\omega(t)\}$. The Hamiltonian is defined in the standard way

$$H_{Dirac}(t) = i\alpha^i(\partial_i - igA_i\mathbf{x}, t)\frac{1-\gamma_5}{2},$$

where $\alpha^i = \gamma^0\gamma^i$, so that the Dirac equation has the Schrödinger form,

$$i\frac{\partial\psi}{\partial t} = H_{Dirac}\psi.$$

We are going to discuss the eigenvalues $\omega(t)$ of the operator $H_{Dirac}(t)$ treating t as a parameter. These eigenvalues ω_n are found from

$$H_{Dirac}(t)\psi_n = \omega_n(t)\psi_n.$$

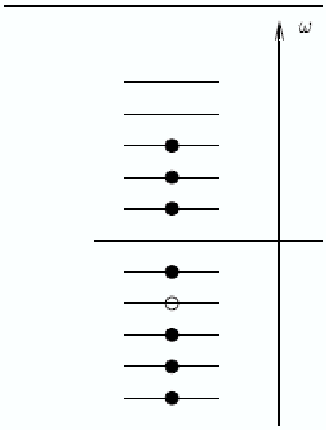

Figure 2: Fermion energy levels at zero background gauge field.

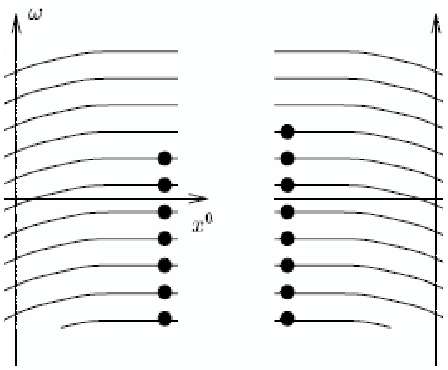

Figure 3: Motion of fermion levels in background gauge fields with non-vanishing Q (shown is the case $Q = 2$). Left panel: left-handed fermions. Right panel: right-handed fermions.

At $\mathbf{A} = 0$ the system of levels is shown schematically in Fig. 2. Importantly, there are both positive- and negative-energy levels. According to Dirac, the lowest energy state (Dirac vacuum) has all negative energy levels filled, and all positive energy levels empty. Occupied positive energy levels (three of them in Fig. 2) correspond to real fermions, while empty negative energy levels describe anti-fermions (one in Fig. 2). Fermion-anti-fermion annihilation is a jump of a fermion from a positive energy level to an unoccupied negative energy level.

In weak background fields, the energy levels depend on time (move), but nothing dramatic happens. For adiabatically varying background fields, the fermions sit on their levels, while fast changing fields generically give rise to jumps from, say, negative- to positive-energy levels, that is, creation of fermion-antifermion pairs. Needless to say, fermion number, $(N_f - N_{\bar{f}})$ is conserved.

The situation is entirely different for the background fields with non-zero Q. The levels of left-handed fermions move as shown in the left panel of Fig. 3. Some levels necessarily cross zero, and the net number of levels crossing zero from below equals Q. This means that the number of left-handed fermions is not conserved: for adiabatically varying gauge fields $\mathbf{A}(\mathbf{x}, t)$ the motion of levels shown in the left panel of Fig. 3 corresponds to the case in which the initial state of the fermionic system is vacuum (no fermions at all) whereas the final state contains Q real fermions (two in the particular case shown). If the evolution of the gauge field is not adiabatic, the result for the fermion number non-conservation is the same: there may be jumps from negative energy levels to positive energy levels, or vice versa. These correspond to creation or annihilation of fermion-antifermion pairs, but the net change of the fermion number (number of fermions minus

number of anti-fermions) remains equal to Q. Importantly, the initial and final field configurations of the gauge field may be $\mathbf{A} = 0$, so that fermion number non-conservation may occur due to a fluctuation that starts from and ends in the gauge field vacuum[12]. This is precisely an instanton-like vacuum fluctuation.

If the same gauge field interacts also with right-handed fermions, the motion of the levels of the latter is opposite to that of left-handed fermions. This is shown in the right panel of Fig. 3. The change in the number of right-handed fermions is equal to $(-Q)$. So, if the gauge interaction is vector-like, the total fermion number $N_{left} + N_{right}$ is conserved, while chirality $N_{left} - N_{right}$ is violated even for massless fermions. This explains why there is no baryon number violation in QCD. On the other hand, non-perturbative violation of chirality in QCD in the limit of massless quarks has non-trivial consequences which are indeed confirmed by phenomenology. In this sense anomalous non-conservation of fermion quantum numbers is an experimentally established fact.

In electroweak theory, right-handed fermions do not interact with $SU(2)_W$ gauge field, while left-handed fermions do. Therefore, fermion number is not conserved. Since fermions of each $SU(2)_W$-doublet interact with the $SU(2)_W$ gauge bosons (essentially W and Z) in the same way, they are equally created in a process involving a gauge field fluctuation with non-zero Q. This again leads to the relations (33) and (34), i.e., to the selection rules

$$\Delta B = \Delta L, \qquad \Delta L_e = \Delta L_\mu = \Delta L_\tau.$$

4.3 Electroweak baryogenesis?

It is tempting to use this mechanism of baryon number non-conservation for explaining the baryon asymmetry of the Universe. There are two problems, however. One is that CP-violation in the Standard Model is too weak: the CKM mechanism alone is insufficient to generate the realistic value of the baryon asymmetry. Hence, one needs extra sources of CP-violation. Another problem has to do with departure from thermal equilibrium that is necessary for the generation of the baryon asymmetry. At temperatures well above 100 GeV electroweak symmetry is restored, the expectation value of ϕ is zero[13], the relation (35) is valid, and the baryon number violation is rapid as compared to the cosmological expansion. At temperatures of order 100 GeV the relation (35) may be violated, but the Universe expands very slowly: the cosmological time scale at these temperatures is

$$H^{-1} = \frac{M^*_{Pl}}{T^2} \simeq \frac{10^{18}\ \text{GeV}}{(100\ \text{GeV})^2} \sim 10^{-10}\ \text{s}, \tag{36}$$

[12] A subtlety here is that in four-dimensional gauge theories, this is impossible for *Abelian* gauge fields, so fermion number non-conservation is possible in *non-Abelian* gauge theories only.

[13] There are subtleties here which are not important for our discussion.

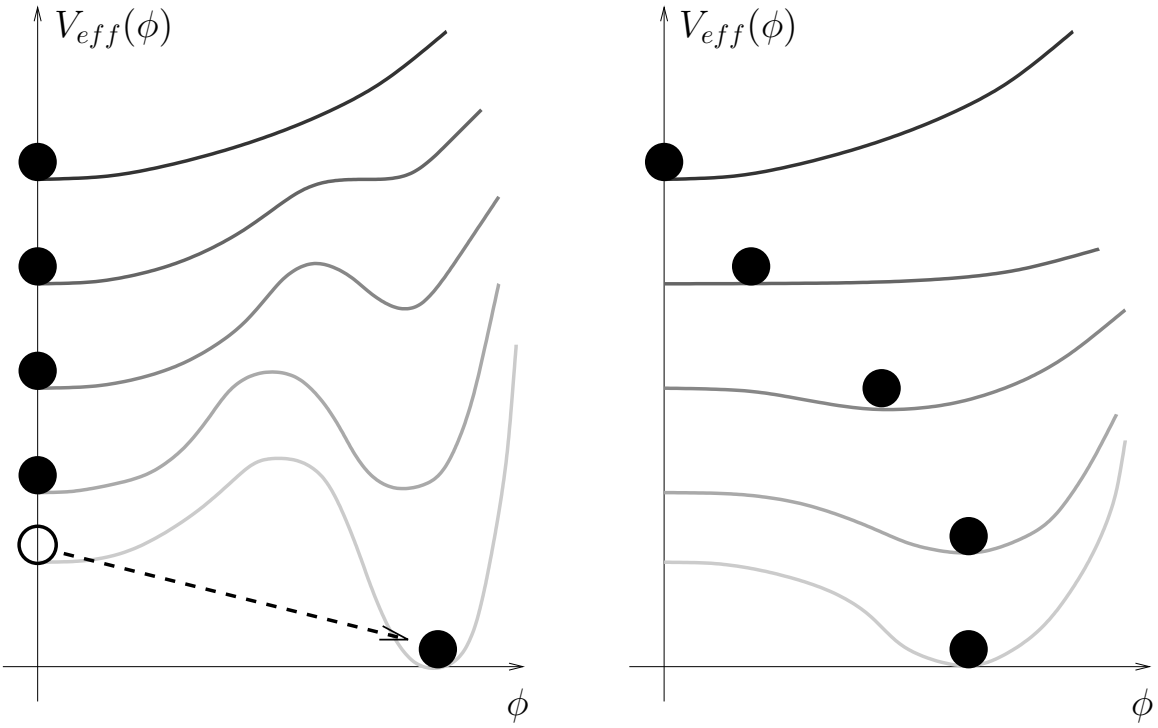

Figure 4: Effective potential as function of ϕ at different temperatures. Left: first order phase transition. Right: second order phase transition. Upper curves correspond to higher temperatures.

which is very large by the electroweak physics standards. The only way strong departure from thermal equilibrium at these temperatures may occur is through the processes happening at the first order phase transition.

The property that at temperatures well above 100 GeV the expectation value of the Higgs field is zero, while it is non-zero in vacuo, suggests that there may be a phase transition from the phase with $\langle\phi\rangle = 0$ to the phase with $\langle\phi\rangle \neq 0$. The situation is pretty subtle here, as ϕ is not gauge invariant, and hence cannot serve as an order parameter, so the notion of phases with $\langle\phi\rangle = 0$ or $\langle\phi\rangle \neq 0$ is pretty vague. In fact, neither electroweak theory nor most of its extensions has a gauge-invariant order parameter, so there is no real distinction between these "phases". The situation here is very similar to that in liquid-vapor system, which does not have an order parameter and may or may not experience vapor-liquid phase transition as temperature decreases, depending on other parameters characterizing this system, e.g., pressure. In the Standard Model the role of such a parameter is played by the Higgs self-coupling λ or, in other words, the Higgs boson mass.

Continuing to use somewhat sloppy terminology, the interesting case for us is the

first order phase transition. In this case the effective potential (free energy density as the function of ϕ) behaves as shown in the left panel of Fig. 4. At high temperatures, there exists one minimum of V_{eff} at $\phi = 0$, and the expectation value of the Higgs field is zero. As the temperature decreases, another minimum emerges at finite ϕ, which then becomes lower than the minimum at $\phi = 0$. However, the probability of the transition from the phase $\phi = 0$ to the phase $\phi \neq 0$ is very small for some time, so the system gets overcooled. The transition occurs when the temperature becomes sufficiently low, as shown schematically by an arrow in Fig. 4. This is to be contrasted to the case, e.g., of the second order phase transition with the behavior of the effective potential shown in the right panel of Fig. 4. In the latter case, the field slowly evolves, as the temperature decreases, from zero to non-zero vacuum value, and the system remains very close to the thermal equilibrium.

The first order phase transition occurs via spontaneous creation of bubbles of the new phase inside the old phase. These bubbles then grow, their wall eventually collide, and the new phase finally occupies entire space. The Universe boils. In the cosmological context, this process happens when the bubble nucleation rate is of order one per Hubble time per Hubble volume,

$$\Gamma_{nucl} \sim H^{-4}.$$

The velocity of the bubble wall in the relativistic cosmic plasma is roughly of the order of the speed of light (in fact, it is somewhat smaller, from 0.1 c to 0.01 c), simply because there are no relevant dimensionless parameters describing the system. Hence, the bubbles grow large before their walls collide: their size at collision is roughly of order of the Hubble size (more precisely, about $0.1H^{-1}$ to $0.01H^{-1}$). While at nucleation the bubble is microscopic – its size is dictated by the electroweak scale and is roughly of order $(100\ \mathrm{GeV})^{-1} \sim 10^{-16}$ cm – its size at collision of walls is macroscopic, $0.1H^{-1} \sim$ a few mm, as follows from (36). Clearly, this boiling is a highly inequilibrium process, and one may hope that the baryon asymmetry may be generated at that time. And, indeed, there exist mechanisms of the generation of the baryon asymmetry, which have to do with interactions of quarks and leptons with moving bubble walls. The value of the resulting baryon asymmetry may well be of order 10^{-10}, as required by observations, provided that there is enough CP-violation in the theory.

A necessary condition for the electroweak generation of the baryon asymmetry is that the inequality (35) is violated *just after* the phase transition. Indeed, in the opposite case the electroweak baryon number violating processes are fast after the transition, and the baryon asymmetry, generated during the transition, is washed out afterwards. Hence, the phase transition must be of strong enough first order. This is *not* the case in the Standard Model. To see why this is so, and to get an idea in which extensions of the Standard Model the transition may be strong enough, let us consider the effective potential in some detail. At zero temperature, the Higgs

potential has the standard form,

$$V(\phi) = -\frac{m^2}{2}|\phi|^2 + \frac{\lambda}{4}|\phi|^4 + \text{const} = \frac{\lambda}{4}\left(|\phi|^2 - v^2\right)^2 .$$

Here

$$|\phi| \equiv \frac{1}{2}\left(\phi^\dagger\phi\right)^{1/2}, \tag{37}$$

and $v = 247$ GeV is the Higgs expectation value in vacuo. The Higgs boson mass is related to the latter as follows,

$$m_H = \sqrt{2\lambda}v. \tag{38}$$

Now, in the leading order of perturbation theory the finite temperature effects modify the effective potential into

$$V_{eff}(\phi, T) = \frac{\alpha}{2}|\phi|^2 - \frac{\beta}{3}T|\phi|^3 + \frac{\lambda}{4}|\phi|^4, \tag{39}$$

with

$$\alpha(T) = -m^2 + \hat{g}^2T^2$$

and

$$\beta = \frac{1}{2\pi}\tilde{g}^3,$$

where $\hat{g}^2$ is a positive linear combination of squares of coupling constants of all fields to the Higgs field (in the Standard Model, a linear combination of g^2, g'^2 and y_i^2, where g and g' are gauge couplings and y_i are Yukawa couplings) while $\tilde{g}^3$ is a positive linear combination of cubes of coupling constants of all *bosonic* fields to the Higgs field. In the Standard Model, β is a linear combination of g^3, g'^3, i.e., a linear combination of M_W^3/v^3 and M_Z^3/v^3,

$$\beta = \frac{1}{2\pi}\frac{2M_W^3 + M_Z^3}{v^3}. \tag{40}$$

The cubic term in (39) is weird: in view of (37) it is not analytic in the original Higgs field ϕ. Yet it is crucial for the first order phase transition: for $\beta = 0$ the phase transition would be of the second order. The origin of the non-analytic cubic term can be traced back to a particular behavior of the Bose–Einstein thermal distribution function at low momenta,

$$f_{Bose}(p) = \frac{1}{\mathrm{e}^{\frac{\sqrt{p^2+m_a^2}}{T}} - 1} \simeq \frac{T}{\sqrt{p^2 + m_a^2}}$$

at $p, m_a \ll T$, where $m_a \simeq g_a|\phi|$ is the mass of the boson a that is generated due to the non-vanishing Higgs field, and g_a is the coupling constant of the field a to the Higgs field. Clearly, at $p \ll g|\phi|$ the distribution function is non-analytic in ϕ,

$$f_{Bose}(p) \simeq \frac{T}{g_a|\phi|}.$$

It is this non-analyticity that gives rise to non-analytic cubic term in the effective potential. Importantly, the Fermi–Dirac distribution

$$f_{Fermi}(p) = \frac{1}{e^{\frac{\sqrt{p^2+m_a^2}}{T}} + 1}$$

is analytic in m_a^2, and hence $\phi^\dagger\phi$, so fermions do not contribute to the cubic term.

With the cubic term in the effective potential, the phase transition is of the first order: at high temperatures the coefficient α is positive and large, and there is one minimum of the effective potential at $\phi = 0$, while for α small but still positive there are two minima. The phase transition occurs at $\alpha \approx 0$; at that moment

$$V_{eff}(\phi, T) \approx -\frac{\beta}{3}|\phi|^3 + \frac{\lambda}{4}|\phi|^4.$$

We find from this expression that immediately after the phase transition the minimum of V_{eff} is at

$$\phi \simeq \frac{\beta}{\lambda} = \frac{\tilde{g}^3 T}{\lambda}.$$

Hence, the necessary condition for successful electroweak baryogenesis, $\phi > T$, translates into

$$\beta > \lambda. \tag{41}$$

According to (38), λ is proportional to m_H^2, whereas in the Standard Model β is proportional to $(2M_W^3 + M_Z^3)$. Therefore, the relation (41) holds for small Higgs boson masses only; in the Standard Model one makes use of (38) and (40) and finds that this happens for $m_H < 50$ GeV, which is ruled out[14].

This discussion indicates a possible way to make the electroweak phase transition strong enough. What one needs is the existence of new bosonic fields that have strong enough coupling to the Higgs field(s), and hence provide large contributions to β. To have an effect on the dynamics of the transition, the new bosons must be present in the cosmic plasma at the transition temperature, $T \sim 100$ GeV, so their masses should not be too high, $M \lesssim 300$ GeV. In supersymmetric extensions of the Standard Model natural candidate is stop whose Yukawa coupling to the Higgs field is the same as that of top, that is, large. The light stop scenario for electroweak baryogenesis indeed works, as has been shown by the detailed analysis in Ref. [11].

Yet another issue is the CP-violation, which has to be strong enough for successful electroweak baryogenesis. As the asymmetry is generated in the interactions of quarks

[14]In fact, in the Standard Model with $m_H > 114$ GeV, there is no phase transition at all; the electroweak transition is smooth crossover instead. The latter fact is not visible from the expression (39), but that expression is the lowest order perturbative result, while the perturbation theory is not applicable for describing the transition in the Standard Model with large m_H.

and leptons (and their superpartners in supersymmetric extensions) with the bubble walls, CP-violation must occur at the walls. Recall now that the walls are made of the Higgs field(s). This points towards the necessity of CP-violation in the Higgs sector, which may only be the case in a theory with more than one Higgs field.

To summarize, electroweak baryogenesis requires considerable extension of the Standard Model, with masses of new particles in the range $100 - 300$ GeV. Hence, this mechanism will definitely be ruled out or confirmed by the LHC. We stress, however, that electroweak baryogenesis is not the only option: an elegant and well motivated competitor is leptogenesis; there are several other mechanisms that may be responsible for the baryon asymmetry of the Universe.

5 What do we know about our Universe and what do we hope to learn?

In this Section we are going to discuss in more detail some known features of our Universe and the prospects for uncovering the unknown properties of the Universe in reasonably near future. In the first place, in our discussion we will assume that the Einstein General Relativity is the correct theory of gravity at all relevant space and time scales. This does not mean that thinking about modifying gravity at large scales (comparable to the present horizon, $l, t \sim H_0^{-1}$) or at small scales (e.g., horizon at inflation) is pointless; in fact, this is an interesting and promising route. Still, at the moment there is no clear evidence for such a modification, so we stick to General Relativity as working hypothesis.

There are two classes of properties that characterize our Universe today and at its early stages. One of these classes has to do with the composition of the Universe and its spatial curvature. We discussed the composition in the previous Sections, and we will have to say more about the spatial curvature later on. The second class has to do with the properties of primordial cosmological perturbations. The latter are extremely important, so let us discuss them now.

5.1 Primordial cosmological perturbations

The Universe is not exactly homogeneous: there are galaxies, clusters of galaxies, gigantic voids, etc. These inhomogeneities originate from small perturbations of energy density and metrics that were somehow built in already at the beginning of the hot stage of the cosmological evolution. The quantitative measurements of the characteristics of these inhomogeneities *in the present and recent Universe* are made precisely by studying the structures and comparing the results with theory. In particular, deep surveys of galaxies and quasars provide a three-dimensional map of the Universe consisting of more than a million objects and extending out to distance of

7000 Mpc (21 billion light years!). Besides this, there are other ways to measure the structure at relatively small redshifts, $z \lesssim 3$ (Lyman-α forest, weak lensing, etc.). On the other hand, the inhomogeneities in the Universe at large redshift $z = 1100$ are observed as angular anisotropy of Cosmic Microwave Background (CMB), as well as its polarization. The variation of the CMB temperature as function of the direction on the sky is very small,

$$\frac{\delta T}{T} \sim 10^{-5} ;$$

this number characterizes the density contrast at the recombination epoch, $z = 1100$. Hence, cosmological perturbations were very small in amplitude at that epoch. Since then they grew: as we already described, overdense regions had attracted surrounding matter and had become even more overdense, until the density contrast became of order of unity, and the non-linear gravitational collapse occurred. In this way the first stars, galaxies and larger gravitationally bound structures were formed.

When the cosmological perturbations are small in amplitude, they can be described within linearized theory about homogeneous and isotropic background. It is then convenient to decompose them into spatial Fourier modes and classify according to their helicities – this is called Lifshits decomposition. Since the linearized Einstein gravity involves fields of spin 2 (graviton) and lower, there are three types of perturbations:

– Scalar perturbations (helicity 0) are perturbations in energy density and associated gravitational potentials. It is this type of perturbations that is responsible for galaxies and other structures; certainly, perturbations of this type exist in our Universe.

– Vector perturbations (helicity 1) correspond to local rotational motion of matter. These have not been observed and are not expected to have existed, at least at relatively late stages of the cosmological evolution. The reason is conservation of angular momentum: as the Universe expands, the distances increase, and because of angular momentum conservation rotational velocities decay.

– Tensor perturbations (helicity 2) are primordial gravitational waves. These have not been observed either, but unlike vector perturbations, they may exist in the Universe and may be detected in reasonably near future. Indeed, sizable amplitude of tensor perturbations is predicted by a class of inflationary models, and if so, effects of tensor perturbations on CMB may be detected.

What do we know about scalar perturbations? At the linear regime, the relevant quantity is the energy density contrast (modulo technicalities),

$$\delta(\mathbf{x}, t) = \frac{\delta\rho(\mathbf{x}, t)}{\overline{\rho}(t)},$$

where $\overline{\rho}$ is the average energy density. The first property is that $\delta(\mathbf{x}, t)$ is *Gaussian*

random field, at least to the first approximation[15].

Let us make spatial Fourier decomposition,

$$\delta(\mathbf{x},t) = \int d^3k\ \mathrm{e}^{i\mathbf{kx}}\delta(\mathbf{k},t), \tag{42}$$

with $\delta^*(\mathbf{k}) = \delta(-\mathbf{k})$ since $\delta(\mathbf{x})$ is real. Note that $\mathbf{x}$ are comoving coordinates, and $\mathbf{k}$ is comoving (conformal) momentum. So, $\mathbf{k}$ is independent of time, while physical momentum $\mathbf{p} = \mathbf{k}/a(t)$ gets redshifted as the Universe expands.

Gaussian random field has the property that its correlators obey what in quantum field theory is known as Wick's theorem,

$$\begin{aligned} \langle\delta(\mathbf{k}_1)\delta(\mathbf{k}_2)\delta(\mathbf{k}_3)\rangle &= 0, \\ \langle\delta(\mathbf{k}_1)\delta(\mathbf{k}_2)\delta(\mathbf{k}_3)\delta(\mathbf{k}_4\rangle &= \langle\delta(\mathbf{k}_1)\delta(\mathbf{k}_2)\rangle\cdot\langle\delta(\mathbf{k}_3)\delta(\mathbf{k}_4)\rangle + \text{ permutations}, \end{aligned}$$

etc. Hence, Gaussian random field is completely characterized by its two-point correlation function. Furthermore, *homogeneous* Gaussian random field is uncorrelated at different momenta, so that

$$\langle\delta(\mathbf{k})\delta^*(\mathbf{k}')\rangle = \frac{P(k)}{(2\pi)^3}\delta(\mathbf{k}-\mathbf{k}'), \tag{43}$$

where by isotropy of the Universe $P(k)$ is a function of $k = |\mathbf{k}|$. The quantity $P(k)$ is called power spectrum; it is the main characteristic of the scalar perturbations in the Universe.

One point to note here: averaging in (43) has to be understood as averaging over *ensemble of universes*. The actual field $\delta(\mathbf{x})$ in our, unique Universe is thus intrinsically unpredictable. To obtain $P(k)$ at relatively small momenta (short spatial scales), one can consider numerous non-overlapping parts of our Universe and average the results to obtain small statistical error. However, at small k this option is not available, so the determination of $P(k)$ is plagued by intrinsic uncertainty, *cosmic variance*.

The power spectrum $P(k)$ is determined at different scales by different methods. To compare the results, one usually converts $P(k,t)$ to the present epoch *by pretending that all perturbations are still in the linear regime*, i.e., by using formulas of the linearized theory. For small momenta (large spatial scales) the latter procedure is unambiguous, since perturbations on these scales are in the linear regime even at the present epoch. On the other hand, perturbations of shorter wavelengths (with present wavelengths $\lambda \lesssim 10$ Mpc) are actually nonlinear today and at small redshift, i.e., at the time they are observed. So, the procedure is as follows. One finds the primordial

[15]Search for non-Gaussianities in the data of observational cosmology is very interesting. There have been several claims for non-Gaussianities in the CMB data, but the issue is still controversial.

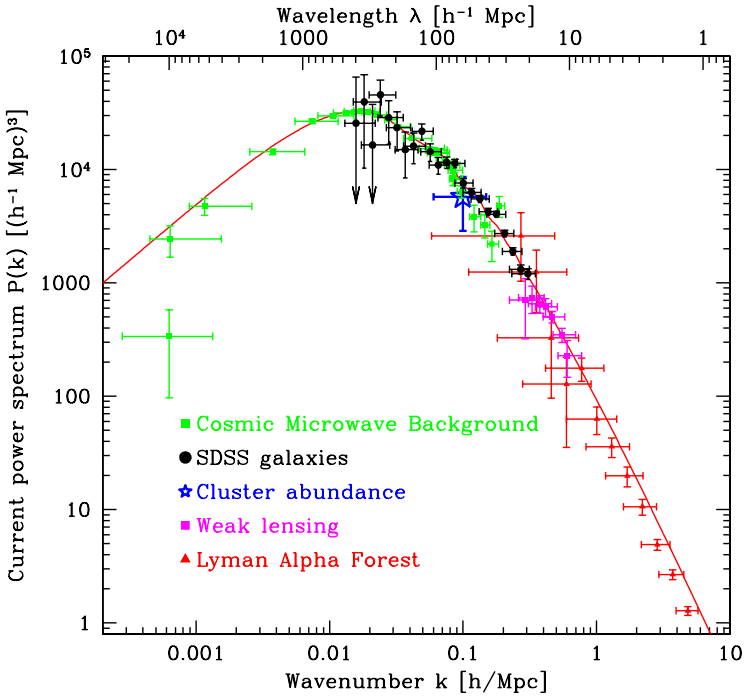

Figure 5: Present power spectrum in linearized theory [12]. Recall that $h \approx 0.7$ is the present Hubble parameter in units 100 km s^{-1} Mpc^{-1}.

power spectrum from the requirement that the observed properties of structure in the Universe are reproduced, and then evolves the primordial perturbations to the present epoch by formally using the linearized theory. The first, difficult part of this procedure requires comparison with non-linear theory. The latter involves numerical simulations of structure formation, and it is believed to be precise enough to make such a comparison meaningful.

The compilation of data on the power spectrum is shown in Fig. 5. Remarkably, different methods give consistent determinations of the spectrum; in particular, observations of large scale structure at low redshift ("SDSS galaxies") are fully consistent with measurements of CMB anisotropy, the latter giving the information on the power spectrum at $z = 1100$. It is also remarkable that the power spectrum does not show any features (except for well understood baryon acoustic oscillations, BAO, not visible in Fig. 5), which implies that the primordial spectrum is very smooth (see below).

It is worth emphasizing that the fact that primordial perturbations are Gaussian

random field can be viewed as a strong hint on their origin. The same property holds for enhanced *vacuum fluctuations* of a linear (non-interacting) scalar field. Indeed, the linear scalar field has the following Fourier decomposition

$$\phi(\mathbf{x},t) = \int \frac{d^3k}{(2\pi)^{3/2}\sqrt{2\omega_k}} \left[\mathrm{e}^{i\mathbf{kx}} f_{\mathbf{k}}^{(+)}(t) a_{\mathbf{k}}^\dagger + \mathrm{e}^{-i\mathbf{kx}} f_{\mathbf{k}}^{(-)}(t) a_{\mathbf{k}} \right], \qquad (44)$$

where creation and annihilation operators obey the standard commutational relation

$$[a_{\mathbf{k}}, a_{\mathbf{k}'}^\dagger] = \delta(\mathbf{k}-\mathbf{k}').$$

In vacuo, positive- and negative-frequency functions are $f_{\mathbf{k}}^{(\pm)}(t) = \exp(\pm\omega_k t)$ This would correspond to perturbations of wrong shape and too small amplitude of $P(k)$. However, vacuum perturbations may get enhanced at early, pre-hot stages of cosmological evolution. This would mean that $f_{\mathbf{k}}^{(\pm)}$ are large. Still, the field (44) would obey Wick's theorem, meaning that its perturbations are Gaussian. This is precisely what happens at inflation; in the simplest scenario the field ϕ is inflation, and its perturbations are in the end converted into scalar cosmological perturbations. Enhancement of vacuum perturbations may occur also in scenarios alternative to inflation; it appears to be a rather general mechanism of the generation of density perturbations in the early Universe.

5.2 Adiabatic mode and isocurvature modes

Matter in the Universe is multi-component. At radiation domination, there is hot component, baryon component and dark matter component. In principle, perturbations in energy densities of these components could have different properties. So, it is useful to classify possible initial conditions for scalar perturbations. This leads to notions of adiabatic mode and isocurvature modes.

Perturbations in the *adiabatic mode* have non-vanishing $\delta\rho$ and δT at early radiation domination epoch, but the chemical composition is the same everywhere in the Universe. The latter property is quantified as

$$\delta\left(\frac{\rho_B}{s}\right) = \delta\left(\frac{\rho_{DM}}{s}\right) = 0.$$

This must be the case if dark matter and baryon asymmetry were generated at the radiation dominated stage: physical processes leading to their generation are the same everywhere in the Universe, so the ratios of number densities of dark matter particles and baryons to that of photons is also the same everywhere. This observation apples to the mechanisms we discussed in previous Sections.

Isocurvature (or entropy) modes, instead, have $\delta T = 0$, so that energy density of dominant, ultra-relativistic component is homogeneous. Since at radiation domination one has $\delta\rho \approx \delta\rho_{rad} \propto \delta T$, there are no metric perturbations early at radiation

dominated stage, hence the term "isocurvature". What varies in space for these modes are energy (mass) densities of baryons or dark matter; for baryon isocurvature perturbations and dark matter isocurvature perturbations one has

$$\delta\left(\frac{\rho_B}{s}\right) \neq 0 \qquad \text{and} \qquad \delta\left(\frac{\rho_{DM}}{s}\right) \neq 0,$$

respectively (hence the term "entropy perturbations"). There can be also neutrino isocurvature modes, but it is hard to design a mechanism that would produce them, and we will not consider them here.

In general, initial condition for scalar perturbations is a linear combination of adiabatic and isocurvature modes. However, as we already pointed out, no admixture of isocurvature modes would exist if baryon asymmetry and dark matter abundance were generated at the hot stage. Conversely, any admixture of isocurvature modes would mean that conventional mechanisms of the generation of baryon asymmetry and/or dark matter are plainly wrong: in that case the generation must have occurred at the same epoch when density perturbations were generated (or earlier), that is, before the hot stage. The latter scenario is not impossible: there are models in which dark matter (e.g., axions) originates from inflationary epoch, and the same for baryon asymmetry (e.g., Affleck–Dine baryogenesis). Still, discovering an admixture of isocurvature mode(s) would be major surprise in astroparticle physics.

At the moment, data are consistent with adiabatic mode only; admixture of isocurvature modes is smaller than about 10%. This has been established by measurements of CMB anisotropy. Further improvements are expected in near future, especially due to Planck experiment. Planck satellite has been launched in May 2009; when looking at Planck data it is worth keeping in mind that a very important outcome could be evidence for isocurvature (entropy) modes.

5.3 Understanding CMB anisotropy

The distribution of CMB on celestial sphere, as seen by WMAP experiment, is shown in Fig. 6. It encodes a lot of physics:

– properties of primordial perturbations built in before the hot stage;

– evolution of perturbations prior to the recombination epoch; in particular, development of sound waves from the early hot stage to recombination;

– propagation of photons after recombination, which is affected, in particular, by the expansion history of the Universe.

To quantify the temperature distribution on celestial sphere, one performs the decomposition in spherical harmonics (the closest analog of the Fourier decomposition),

$$\delta T(\theta, \varphi) = \sum_{lm} a_{lm} Y_{lm}(\theta, \varphi).$$

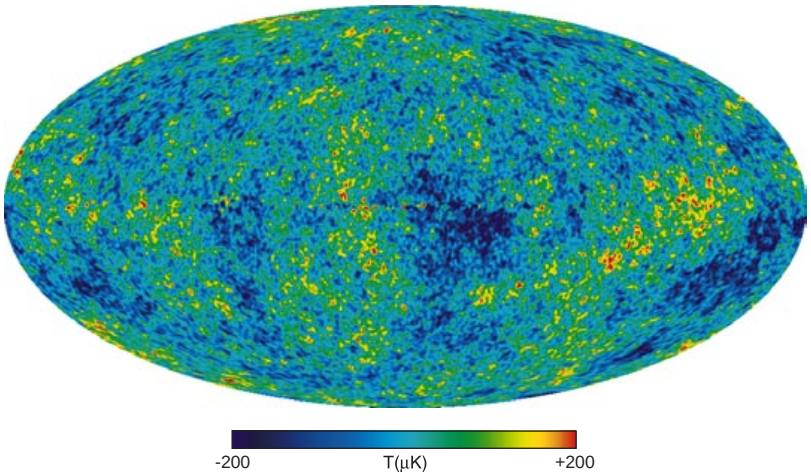

Figure 6: CMB sky. The isotropic component ($T = 2.725$ K) and dipole component ($\delta T = 3.346$ mK) are subtracted – the latter is due to the motion of the Earth with respect to CMB. The residual anisotropy is at the level of 100 μK, i.e., $\delta T/T \sim 10^{-4} - 10^{-5}$.

If cosmological perturbations are Gaussian random field(s), the coefficients a_{lm} are independent Gaussian random variables (they are linear functions of $\delta\rho/\rho$). Their correlator vanishes for different indices,

$$\langle a_{lm} a^*_{l'm'} \rangle \propto \delta_{ll'} \delta_{mm'},$$

so all information is contained in

$$\langle a_{lm} a^*_{lm} \rangle \equiv C_l \tag{45}$$

(because of rotational symmetry, the left hand side here is independent of m). The coefficients C_l are measured; what is usually shown is

$$D_l = \frac{l(l+1)}{2\pi} C_l.$$

Larger values of l correspond to smaller angular scales, and hence shorter wavelengths of perturbations.

In fact, one cannot measure the average over an ensemble of universes, and the actually measured quantity is

$$C_l = \frac{1}{2l+1} \sum_m |a_{lm}|^2$$

for a single, our realization of the random field $\delta T(\theta, \varphi)$. This is of course different from (45), and the intrinsic statistical error – cosmic variance – is

$$\frac{\Delta C_l}{C_l} \simeq \frac{1}{\sqrt{2l}}.$$

For large l this error is small, but it becomes sizable and important for low multipoles.

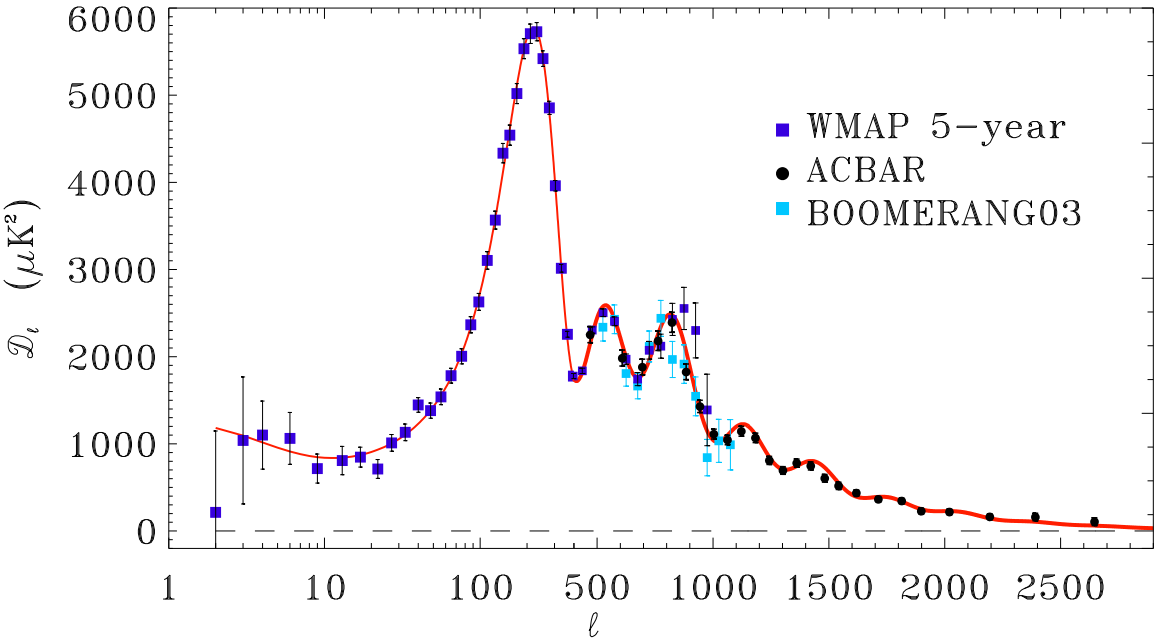

Figure 7: Compilation of data on CMB temperature anisotropy made by collaboration ACBAR [13]. Note peculiar scale on horizontal axis. Error bars at low multipoles are not experimental: they are due to cosmic variance.

One compilation of the data is shown in Fig. 7. Let us give an idea of physics behind this plot.

In the first place, effects of tensor perturbations have not been observed so far (details are given below). So, we assume here that the entire temperature anisotropy is due to scalar perturbations.

Baryon-electron-photon component is a single fluid before recombination, because of strong interaction of photons with free electrons, and Coulomb interaction between electrons and protons. Perturbations in this component are sound waves propagating in the plasma. For *adiabatic mode* the density contrast oscillates as follows:

$$\text{Baryon–electron–photon}: \qquad \frac{\delta\rho}{\rho}(k,t) \propto \cos\left(\int_0^t dt\, \frac{v_s(t)k}{a(t)}\right), \qquad (46)$$

where $k/a(t)$ is the physical momentum, $v_s(t)$ is sound velocity and $v_s k/a$ is physical frequency. It turns out that *the phase of these oscillations is fixed* precisely as indicated in (46). For isocurvature perturbations the phase is different; for short enough waves the phase shift is $\pi/2$. This difference in the behaviour enables one disentangle adiabatic and isocurvature perturbations, and set the bound on the latter, which we discussed above.

Dark matter is pressureless well before recombination. Because of that, perturbations in dark matter do not oscillate. As far as baryon-electron-photon component is concerned, dark matter perturbations produce gravitational potentials for it.

The temperature anisotropy emerges due to four effects. Three of them occur at recombination epoch[16]:

– Photon energy density is related to temperature as $\rho_\gamma \propto T^4$. Hence, perturbations in baryon-electron-photon component give rise to perturbations of temperature at recombination (more precisely, at the time of last scattering of photons off electrons),

$$\frac{\delta T}{T} = \frac{1}{4}\frac{\delta\rho_\gamma}{\rho_\gamma}(t_{rec}). \tag{47}$$

– Perturbations in the gravitational potential Φ at recombination induce perturbations of temperature of photons we see today: if the potential is negative, photons have to climb gravitational well, and hence they loose energy, and vice versa. This gives the contribution

$$\frac{\delta T}{T} = \Phi(t_{rec}). \tag{48}$$

In this way dark matter perturbations affect CMB temperature; gravitational potentials due to perturbations in baryon-electron-photon component are non-negligible too, although they are subdominant (by recombination, most of the energy density resides in dark matter).

– Motion of baryon-electron-photon plasma in sound waves gives rise to Doppler effect, hence

$$\frac{\delta T}{T} = v_{\gamma\,||}(t_{rec}) \propto d\rho_\gamma/dt, \tag{49}$$

where $v_{\gamma\,||}$ is the velocity along the line of sight.

The first two contributions are jointly called Sachs–Wolfe effect, while the third one is called Doppler effect.

Finally, when travelling from the surface of last scattering to us, photons may loose or gain energy, depending on the distribution of gravitational potential along

[16]At short wavelengths, i.e., large multipoles, important effects are due to relatively large mean free path of photons at the epoch of their last scattering. These effects – Silk damping, finiteness of the width of the sphere of last scattering, etc. – tend to wash out the temperature anisotropy. This is seen in Fig. 7: anisotropy decreases with l at $l \gtrsim 1000$.

their path. This gives rise to *integrated Sachs–Wolfe effect*[17]

$$\frac{\delta T}{T} = 2\int dt \frac{\partial \Phi}{\partial t}, \tag{50}$$

where integration runs along the photon path (the integrand is not total derivative, the total derivative along the photon path is equal to $d\Phi/dt = \partial\Phi/\partial t + \mathbf{n}\nabla\Phi$ where $\mathbf{n}$ is the direction of photon travel).

The resultant temperature anisotropy is the sum[18] of (47), (48),(49) and (50). For what follows, it is important to note that the Doppler effect and integrated Sachs–Wolfe effect are subdominant, and to zeroth approximation the CMB temperature anisotropy is the sum of (47) and (48). In any case, by measuring the CMB temperature anisotropy (and polarization) one learns a lot about the early and present Universe. Let us give a few examples.

Positions of peaks in the CMB angular spectrum provide the standard ruler back at recombination epoch. Indeed, these peaks are due to the fact that according to (46), modes of a certain wavelength develop large value of $|\delta\rho_\gamma|$ by recombination, while others are at the minimum of $|\delta\rho_\gamma|$ at that time. The peaks in the angular spectrum correspond to angular sizes of modes at maximum of $|\delta\rho_\gamma|$, i.e. modes of conformal momentum k_n obeying

$$\int_0^{t_{rec}} dt\ \frac{v_s(t)k_n}{a(t)} = \pi n, \qquad n = 1, 2, \ldots$$

The sound velocity in the baryon-electron-photon plasma is readily calculable (it slightly depends on baryon-to-photon ratio, but the latter is determined with high precision from other properties of the CMB angular spectrum, see below), the time dependence of the scale factor is also well known, so these values of k (and hence the wavelengths at recombination) are well determined. This is precisely what is meant by standard ruler. The angular size of this standard ruler strongly depends on spatial curvature (and to less extent on dark energy density Ω_Λ): the same interval is seen on a sphere at larger angle as compared to plane. In this way one infers the spatial curvature; as we already mentioned, it has been found that our space is Euclidean to high precision.

Heights of peaks are very sensitive to baryon number density. If not for baryons, the two contributions to the Sachs–Wolfe effect, eqs. (47) and (48), would partially cancel each other. It is in this way that the baryon-to-photon ratio is measured by CMB observations at high precision.

[17] We slightly oversimplify the discussion here. Note that the factor 2 in (50) is relativistic effect, just as in the case of the photon propagation near the Sun.

[18] We do not discuss here one more effect which is due to re-ionization of cosmic medium at $z \sim 10$, the time at which the first stars form. This effect is small but important at the current level of precision of observations; it affects particularly strongly CMB polarization.

Of course, the CMB angular spectrum is sensitive to properties of primordial perturbations, that is, initial data for the evolution of inhomogeneities in the Universe. At the very early cosmological stage (but already at radiation domination era), the Universe expands so fast that perturbations do not have time to evolve. So, primordial perturbations are characterized by time-independent power spectrum. Let us consider adiabatic perturbations and introduce convenient notation,

$$\mathcal{P}_s(k) = \frac{k^3 P_{init}(k)}{2\pi^2},$$

where $P_{init}(k)$ is primordial power spectrum of scalar perturbations. The meaning of $\mathcal{P}_s(k)$ is best understood by considering the fluctuation of the density contrast at a given point in space. Making use of eqs. (42) and (43), we find

$$\langle \delta^2 \mathbf{x} \rangle = \int_0^\infty \frac{dk}{k}\, \mathcal{P}_s(k),$$

where integration runs over modulus of spatial momentum. Hence, $\mathcal{P}_s(k)$ gives the contribution of a logarithmic interval of momenta into the fluctuation. It is traditional to parametrize the primordial power spectrum as follows,

$$\mathcal{P}_s(k) = A_s \left(\frac{k}{k_*}\right)^{n_s - 1}. \tag{51}$$

Here A_s is the scalar amplitude, k_* is some fiducial value of conformal momentum (the choice of WMAP is $k_*/a_0 = (500\ \mathrm{Mpc})^{-1}$) and n_s is the scalar spectral index. We will discuss the simplest parametrization in which n_s is independent of k, though weak dependence of n_s on k is also often included into fits by writing $n_s(k) = n_s(k_*) + (dn_s/d\ln k)\cdot \ln(k/k_*)$. The reference point is $n_s = 1$, that is flat, Harrison–Zeldovich spectrum. $n_s < 1$ and $n_s > 1$ correspond to red and blue tilted spectra, producing more power at low and high multipoles, respectively. Inflationary scenarios typically predict a few per cent tilt, $(n_s - 1) \sim (\text{a few})\cdot 10^{-2}$, whose sign depends on a particular model of inflation.

Inflationary models often predict also sizable tensor modes. These are parametrized in analogy to (51) (definitions of the spectral index here and in (51) are a matter of tradition),

$$\mathcal{P}_T(k) = A_T \left(\frac{k}{k_*}\right)^{n_T}.$$

In the simplest models of inflation the tensor amplitude A_T is somewhat smaller than the scalar one, but not very much smaller. In terms of the ratio

$$r = \frac{A_T}{A_s}$$

this means that the prediction of these models is in the range $r \sim (\text{a few}) \cdot 10^{-1}$. It is worth noting that alternatives to inflation typically do not predict sizable amplitude of tensor perturbations, so the discovery of tensor modes would be a very strong argument in favor of inflation.

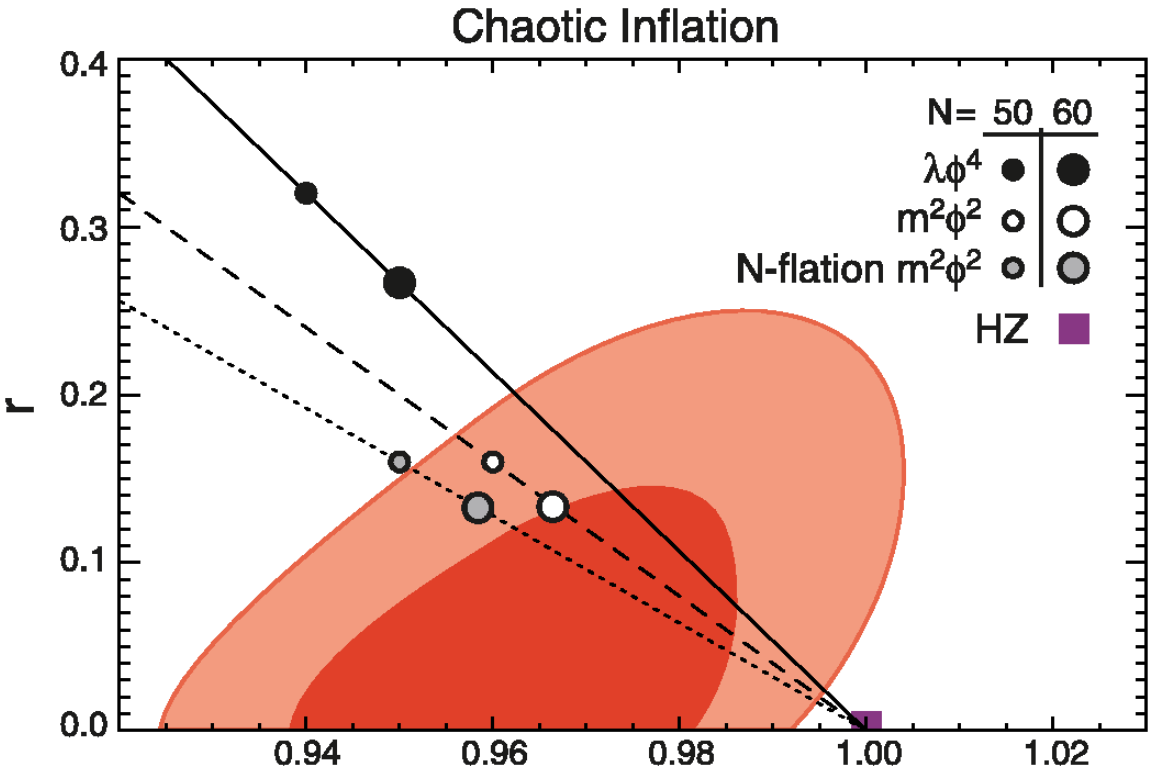

Figure 8: Regions in (n_s, r) plane allowed at 1σ and 2σ level [7]. Small circles correspond to various inflationary models with different number of e-foldings N. Square shows the Harrison–Zeldovich point $n_s = 1$, $r = 0$.

The present observational situation is summarized in Fig. 8. Tensor perturbations would enhance the CMB angular spectrum mostly at low multipoles (amplitude of gravitational waves decays as a^{-1}, starting from the time when $k/a(t) \sim H(t)$; hence, high momentum modes are suppressed by recombination, while low momentum modes are not). Similar effect would be produced by red scalar tilt, $n_s < 1$. Observational data appear to favor more power at low multipoles, which is an indication of either red tilt or admixture of tensor modes, or both. This result is still not conclusive; the situation may change dramatically in near future.

Further opportunity to detect tensor perturbations – relic gravitational waves – comes from the fact that they produce very specific polarization pattern in CMB, which cannot be due to scalar perturbations. Not going into details, we mention

that there are two possible types of polarization, called E- and B-modes. Scalar perturbations produce polarization in E-mode, and this effect has been observed. Tensor perturbations give rise to B-mode (together with E-mode), whose observation would mean the discovery of primordial gravity waves. It goes without saying that this would be an event of utmost importance.

5.4 Neutrino masses and cosmology

One more aspect of cosmology related to particle physics is the effect of neutrino on structure formation in the Universe. Neutrino number density in comoving volume freezes out at temperature 2−3 MeV, when electrons and positrons are still relativistic, and hence abundant in the plasma. After that (at $T \lesssim m_e = 0.5$ MeV) electron-positron annihilation heats up the photon component, while neutrino component does not feel this effect. Hence, effective temperature of neutrinos at $T \ll m_e$ is somewhat smaller than temperature of photons, and the number density of each type of neutrinos is quite a bit smaller than that of photons. Without going into details, we again quote the result for the present number density of neutrinos,

$$n_{\nu_1} = n_{\nu_2} = n_{\nu_3} = 112 \text{ cm}^{-3},$$

where ν_i denote neutrino mass eigenstates.

Neutrino oscillation data imply that if neutrinos are heavier than 0.1 eV, they are degenerate in mass. Relatively heavy neutrinos would make rather large portion of dark matter. As an example, for $m_\nu = 0.3$ eV the present mass density of neutrinos is

$$\rho_{\nu,total} = 3 \cdot 0.3 \text{ eV} \cdot 112 \text{ cm}^{-3} = 10^{-7} \text{ GeV} \cdot \text{cm}^{-3} = 0.1\rho_{DM,0}, \qquad (52)$$

where we used the estimate for the present dark matter density $\rho_{DM,0} \approx 0.2\rho_c = 0.2 \cdot 5 \cdot 10^{-6}$ GeV cm^{-3}. The estimate (52) shows that effect of neutrinos on stricture formation may indeed be sizable.

Neutrino is *hot* component of dark matter. Repeating the discussion in the beginning of Section 3.2, we find that neutrinos tend to wash out structures up to very large size. The predictions for power spectrum for various neutrino masses and the observational data are shown in Fig. 9. It is clear from this figure that heavy neutrinos suppress the density perturbations too strongly, and hence they are inconsistent with cosmology. Different authors obtain different bounds on neutrino masses; we give here a fairly conservative bound [7],

$$\sum_i m_{\nu_i} < 0.6 \text{ eV},$$

meaning that the mass of each neutrino spices is bounded by $m_\nu < 0.2$ eV. This is stronger than experimental bounds. Interestingly, the progress in cosmological obser-

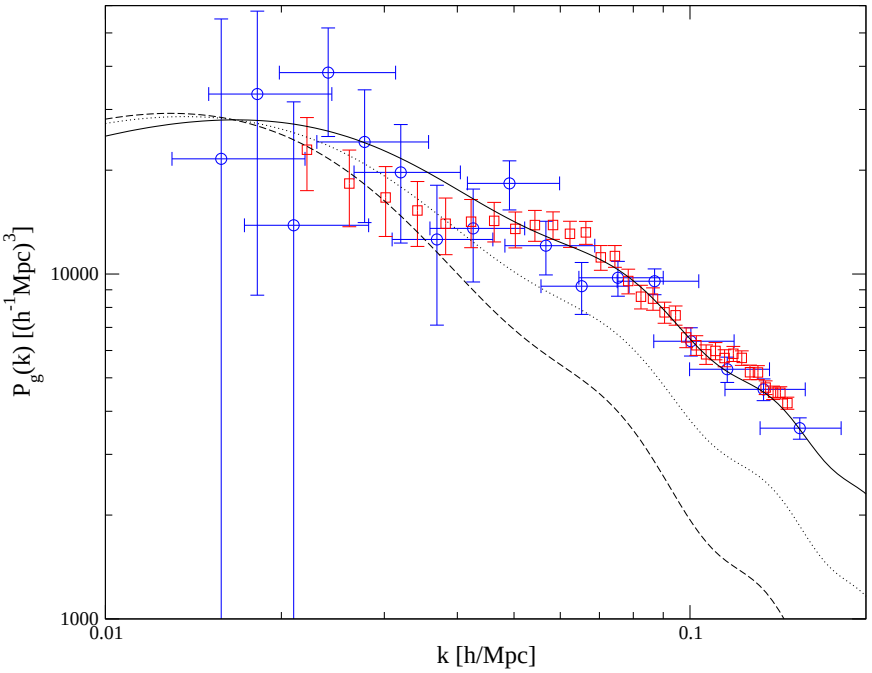

Figure 9: Predictions for the power spectrum for mass of each neutrino spices equal to 0.09 eV (solid line), 0.5 eV (dotted line) and 1 eV (dashed line), and their comparison with data [14].

vations (and in theory of structure formation) may lead to cosmological determination of neutrino mass before its experimental measurement.

5.5 Dark energy

Dark energy is probably the most mysterious form of energy in our Universe; its discovery was a shock to many particle physicists. By definition, dark energy density either does not change in time at all, or changes very slowly, much slower than, say, the energy (mass) density of non-relativistic matter. Because of that, the Hubble parameter also changes in time slowly. Indeed, according to eq. (17), for constant in time $\rho = \rho_\Lambda$ the Hubble parameter would not change in time at all.

Dark energy shows up in the Universe exclusively through the expansion rate at late times. This in turn affects the distance-redshift relation: for given present value of the Hubble parameter H_0, the Universe with dark energy expands faster in the recent past, so the distance to objects of given redshift is larger as compared to the Universe without dark energy. This is shown in Fig. 10. Note that the effect similar to dark energy may be produced by negative spatial curvature; however, this is not

an option since, as we discussed above, CMB data show that the spatial curvature of our Universe is either zero or very close to zero.

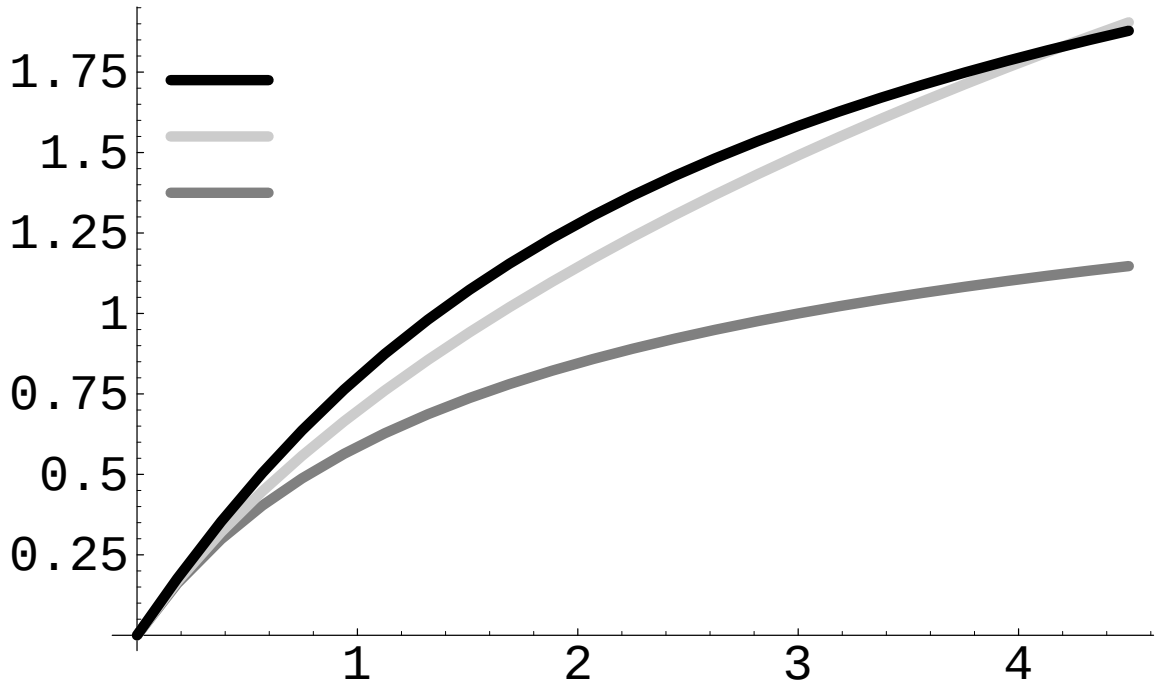

Figure 10: Distance-redshift relation for different cosmological models: $\Omega_M = \Omega_{DM} + \Omega_B = 0.24$, $\Omega_\Lambda = 0.76$, $w_{DE} = -1$ (black line); $\Omega_M = 1$, $\Omega_\Lambda = 0$ (dark gray line); $\Omega_M = 0.24$, $\Omega_\Lambda = 0$, negative spatial curvature (light gray line).

One way to measure the redshift-distance relation is to make use of "standard candles", objects whose absolute luminosity is assumed to be known. Then the distance to a given object is found simply by measuring its visible luminosity, while measuring its redshift is a standard (and accurate) procedure in astronomy. The standard candles used in practice are supernovae of type 1a (SNe1a); their observations show that they are significantly dimmer than what one would expect in the Universe without dark energy (see Refs. [9, 15] for reviews).

It is important to note that SNe1a are not the only probes of dark energy: there are independent (but less precise) ways to measure the dark energy density. As an example, rapid expansion of the Universe filled with dark energy suppresses formation of structure at late times. The strongest effect occurs for clusters of galaxies which are formed only recently. This effect has indeed been observed, see Fig. 11; note that these observations disentangle the dark energy and spatial curvature. Dark energy affects also CMB temperature anisotropy, its correlation with large scale structure

(via integrated Sachs–Wolfe effect), etc. One likes it or not, the existence of dark energy in our Universe is a fact[19].

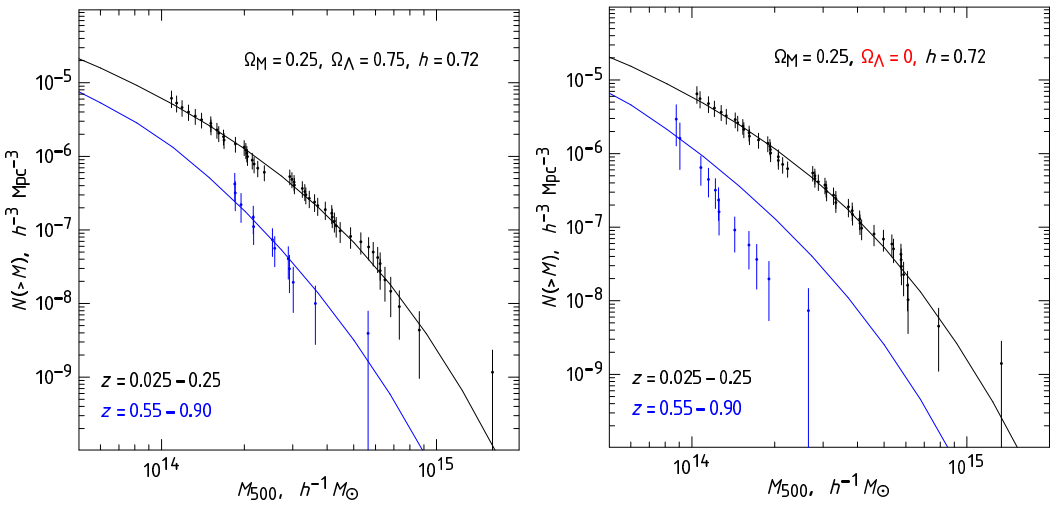

Figure 11: Abundance of clusters of galaxies (number density of clusters with mass greater than shown on horizontal axis) at different redshifts in the Universe with dark energy (left panel) and in the Universe without dark energy but with negative spatial curvature (right panel) [16].

To quantify what we know about dark energy, let us begin with the general expression for the energy-momentum tensor of any kind of matter in homogeneous isotropic case (in locally Lorentz frame),

$$T_{\mu\nu} = \mathrm{diag}(\rho, p, p, p),$$

where ρ is energy density and p is (effective) pressure. It is convenient to parametrize the relation between pressure and energy density (effective equation of state) as follows,

$$p = w\rho,$$

where the parameter w may depend on time. Elementary application of the first law of thermodynamics in the expanding Universe gives the rate at which energy density changes:

$$\dot\rho = -3\frac{\dot a}{a}(\rho + p) = -3(1 + w)\frac{\dot a}{a}.$$

[19]This is true within General Relativity. The observational fact is that the expansion of the Universe accelerates. An alternative explanation of this phenomenon would be the modification of General Relativity at cosmological scales; there has been quite an activity in the latter direction in recent years.

Hence, dark energy density does not change in time at all if $w_{DE} = -1$, i.e., $p_{DE} = -\rho_{DE} \equiv -\rho_\Lambda$. This is the case for vacuum energy density (or cosmological constant, which is the same thing at least with present understanding of this issue). Indeed, by Lorentz-invariance the vacuum energy-momentum tensor in locally Lorentz frame is equal to

$$T^{vac}_{\mu\nu} = \rho_\Lambda \cdot \eta_{\mu\nu},$$

where $\eta_{\mu\nu}$ is Minkowski tensor, and ρ_Λ is independent of time – this is a fundamental constant of Nature. The problem with vacuum as dark energy is that the value of ρ_Λ is ridiculously small by particle physics standards: $\rho_\Lambda = (2 \cdot 10^{-3}\ \mathrm{eV})^4$. Explaining so small value is a problem which has not been solved (except for anthropic argument, see Ref. [17]).

Another possibility is that the dark energy is the energy of some light field. If this is more or less usual field (modulo energy scale which remains unexplained), then $w_{DE} > -1$, and dark energy density decreases in time. Such a field is generically called quintessence. More exotic is phantom, field whose energy density *increases in time* despite the expansion of the Universe; phantom has $w_{DE} < -1$. Generically, phantom fields have instabilities, but time scale for an instability may be very long, so it may not get developed our expanding Universe. Both for quintessence and phantom, the equation of state parameter w_{DE} changes in time; in many concrete models this is slow change, $|\dot{w}_{DE}| \lesssim H_0$, i.e., $|dw_{DE}/dz| \lesssim 1$.

The current situation with observations is as follows. If the parameter w is allowed to change in time, its present value is within the range [7]

$$-1.4 < w_{DE,0} < -0.8,$$

while $w'_{DE} = dw_{DE}/dz$ is bounded by

$$-0.5 < w'_{DE} < 1.5.$$

Hence, significant deviation from vacuum equation of state is still allowed, and the entire situation is presently rather uncertain.

5.6 What do we hope to learn from cosmological observations

It is clear from the above discussion that there are many questions which still have not been answered by observations, and which will hopefully be clarified by future cosmological data. Some of these questions have to do with properties of primordial perturbations, and some have to do with matter content in our Universe. Let us summarize them.

1. The questions on primordial perturbations include:

1.1. Is there tilt in the scalar spectrum? The tilt is predicted by most models of inflation and many alternatives to inflation. It is even somewhat alarming that the tilt is so low that its decisive determination has not been made yet.

1.2. Are there primordial gravity waves? Many (but by no means all) inflationary models predict sizable amplitude of tensor perturbations. Their discovery would be a very strong argument for inflation, especially if the tensor spectrum would be nearly flat.

1.3. Are there isocurvature (entropy) scalar perturbations? These should not exist for currently popular models in which the generation of dark matter and baryon asymmetry occur at the hot stage. Conversely, if an admixture of isocurvature perturbations is found, no matter how small, dark matter and/or baryon asymmetry generation would be shifted to pre-hot stage, like late inflationary epoch or reheating epoch just after inflation.

1.4. Are scalar perturbations Gaussian? Simple models of the generation of primordial perturbations, in which they originate from vacuum fluctuations of inflation field, predict very low level and specific form of non-Gaussianity. However, in more complicated models non-Gaussianity may be much stronger, and its character may be quite different.

All these issues are fascinating, as they have to do with very early, pre-hot stage of the cosmological evolution. We hope to open soon the window to the very first instants of our Universe.

2. Composition of the Universe is of particular interest to particle physics. The unsolved questions include:

2.1. Is dark matter cold or warm? The answer to this question is crucial for choosing between dark matter particle candidates and mechanisms of dark matter generation in the early Universe.

2.2. Is dark energy constant in time? Dark energy density is time-independent if and only if it is vacuum energy = cosmological constant. Observation of time dependence of the dark energy density would mean that dark energy is due to new light, very weakly interacting field – quintessence or phantom, or (and?) General Relativity is not valid at cosmological scales.

2.3. How large are neutrino masses? Interestingly, this question may first be answered by cosmology, and only later by particle physics experiment.

Of course, there is always room for something unexpected – and hence even more interesting!

6 Concluding remarks

The ideas we discussed in these lectures may well be not the right ones: we can only hypothesize on physics beyond the Standard Model and its role in the early Universe. TeV scale physics may be dramatically different from physics we get used to. As an example, it is not excluded that TeV is not only electroweak, but also gravitational scale. This is the case in models with large extra dimensions, in which

the Planck scale is related to the fundamental gravity scale in a way that involves the volume of extra dimensions, and hence the fundamental scale can be much below M_{Pl} (for reviews see, e.g., Ref. [18]). If the LHC will find that, indeed, the fundamental gravity scale is in the TeV range, this would have most profound consequences for both microscopic physics and cosmology. On the microscopic physics side, this would enable one to study quantum gravity and its high-energy extension at colliders, while on the cosmological side, the entire picture of the early Universe will have to be revised. The highest temperatures in the usual expansion history would in that case be at most at TeV range, so dark matter and baryon asymmetry generation would have to occur either below those temperatures or in quantum gravity regime. Even more intriguing will be the study of quantum gravity cosmological epoch, with hints from colliders on quantum gravity gradually coming. This, probably, is too bright a prospective to hope for it seriously.

It is more likely that the LHC will find something entirely new, something theorists have not thought about. Or, conversely, find so little that one will have to get serious about anthropic principle. In any case, the LHC results together with new cosmological observations will definitely change the landscape of both particle physics and cosmology.

Bibliography

[1] E.W. Kolb and M.S. Turner, *The Early Universe,* Addison-Wesley, Redwood City, 1990 – Frontiers in physics, 69;
V. Mukhanov, *Physical Foundations of Cosmology*, Cambridge University Press, 2005;
D.S. Gorbunov and V.A. Rubakov, *Introduction to the Theory of the Early Universe. Hot Big Bang Theory*, URSS, Moscow, 2008 (in Russian).

[2] R.H. Brandenberger, *Particle physics aspects of modern cosmology,* arXiv:hep-ph/9701276;
W.L. Freedman and M.S. Turner, *Measuring and understanding the Universe,* Rev. Mod. Phys. **75** (2003) 1433 [arXiv:astro-ph/0308418];
V. Rubakov, *Introduction to cosmology,* PoS **RTN2005** (2005) 003 ;
J.A. Peacock, *Cosmology and particle physics,* Proc. 1998 European School of High-Energy Physics, St. Andrews, Scotland, 23 Aug - 5 Sep 1998;
M. Shaposhnikov, *Cosmology and astrophysics,* Proc. 2000 European School of High-Energy Physics, Caramulo, Portugal, 20 Aug - 2 Sep 2000;
I.I. Tkachev, *Astroparticle physics,* Proc. 2003 European School on High-Energy Physics, Tsakhkadzor, Armenia, 24 Aug - 6 Sep 2003, arXiv:hep-ph/0405168.

[3] G. Jungman, M. Kamionkowski and K. Griest, *Supersymmetric dark matter,* Phys.

Rept. **267** (1996) 195 [arXiv:hep-ph/9506380];
A. Bottino and N. Fornengo, *Dark matter and its particle candidates,* arXiv:hep-ph/9904469;
K.A. Olive, *Dark matter,* arXiv:astro-ph/0301505;
G. Bertone, D. Hooper and J. Silk, *Particle dark matter: evidence, candidates and constraints,* Phys. Rept. **405** (2005) 279. [arXiv:hep-ph/0404175].

[4] A.D. Dolgov, *Baryogenesis, 30 years after,* arXiv:hep-ph/9707419
V.A. Rubakov and M.E. Shaposhnikov, *Electroweak baryon number non-conservation in the early universe and in high-energy collisions,* Usp. Fiz. Nauk **166** (1996) 493 [Phys. Usp. **39** (1996) 461] [arXiv:hep-ph/9603208];
A. Riotto and M. Trodden, *Recent progress in baryogenesis,* Ann. Rev. Nucl. Part. Sci. **49** (1999) 35 [arXiv:hep-ph/9901362];
M. Trodden, *Electroweak baryogenesis,* Rev. Mod. Phys. **71** (1999) 1463 [arXiv:hep-ph/9803479].

[5] A. de Oliveira-Costa, G.F. Smoot and A.A. Starobinsky, *Constraining topology with the CMB,* arXiv:astro-ph/9705125;
W.N. Colley and J.R.I. Gott, *Genus Topology of the Cosmic Microwave Background from WMAP,* Mon. Not. Roy. Astron. Soc. **344**, 686 (2003) [arXiv:astro-ph/0303020];
N.G. Phillips and A. Kogut, *Constraints On The Topology Of The Universe From The WMAP First-Year Sky Maps* Astrophys. J. **645**, 820 (2006) [arXiv:astro-ph/0404400];
J.R.I. Gott, W.N. Colley, C.G. Park, C. Park and C. Mugnolo, *Genus Topology of the Cosmic Microwave Background from the WMAP 3-Year Data,* arXiv:astro-ph/0610764.

[6] E. Gawiser and J. Silk, *The Cosmic Microwave Background Radiation,* Phys. Rept. **333**, 245 (2000) [arXiv:astro-ph/0002044].

[7] E. Komatsu *et al.* [WMAP Collaboration], *Five-Year Wilkinson Microwave Anisotropy Probe (WMAP) Observations:Cosmological Interpretation,* arXiv:0803.0547 [astro-ph].

[8] U. Seljak *et al.* [SDSS Collaboration], *Cosmological parameter analysis including SDSS Ly-alpha forest and galaxy bias: Constraints on the primordial spectrum of fluctuations, neutrino mass, and dark energy,* Phys. Rev. D **71**, 103515 (2005) [arXiv:astro-ph/0407372].

[9] V. Sahni and A. Starobinsky, *The Case for a Positive Cosmological Lambda-term,* Int. J. Mod. Phys. D **9** (2000) 373 [arXiv:astro-ph/9904398].

[10] V.A. Rubakov, *Classical Gauge Fields*, URSS, Moscow, 1999 (in Russian);
V.A. Rubakov, *Classical Gauge Fields. Theories with Fermions. Noncommutative Theories*, URSS, Moscow, 2009 (in Russian);
V.A. Rubakov, *Classical Theory of Gauge Fields*, Princeton University Press, 2002.

[11] M.S. Carena, M. Quiros and C.E.M. Wagner, *Opening the Window for Electroweak Baryogenesis,* Phys. Lett. B **380** (1996) 81 [arXiv:hep-ph/9603420];
M.S. Carena, M. Quiros, A. Riotto, I. Vilja and C.E.M. Wagner, *Electroweak baryogenesis and low energy supersymmetry,* Nucl. Phys. B **503** (1997) 387 [arXiv:hep-ph/9702409];
M.S. Carena, M. Quiros, M. Seco and C.E.M. Wagner, *Improved results in supersymmetric electroweak baryogenesis,* Nucl. Phys. B **650** (2003) 24 [arXiv:hep-ph/0208043].

[12] M. Tegmark *et al.* [SDSS Collaboration], *The 3D power spectrum of galaxies from the SDSS,* Astrophys. J. **606** (2004) 702 [arXiv:astro-ph/0310725].

[13] C.L. Reichardt *et al.*, *High resolution CMB power spectrum from the complete ACBAR data set,* arXiv:0801.1491 [astro-ph].

[14] V. Barger, D. Marfatia and A. Tregre, *Neutrino mass limits from SDSS, 2dFGRS and WMAP,* Phys. Lett. B **595** (2004) 55 [arXiv:hep-ph/0312065].

[15] T. Padmanabhan, *Cosmological constant: The weight of the vacuum,* Phys. Rept. **380** (2003) 235 [arXiv:hep-th/0212290] ;
P.J.E. Peebles and B. Ratra, *The cosmological constant and dark energy,* Rev. Mod. Phys. **75** (2003) 559 [arXiv:astro-ph/0207347] ;
V. Sahni, *Dark matter and dark energy,* Lect. Notes Phys. **653** (2004) 141 [arXiv:astro-ph/0403324] ;
V. Sahni and A. Starobinsky, *Reconstructing dark energy,* Int. J. Mod. Phys. D **15** (2006) 2105 [arXiv:astro-ph/0610026].

[16] A. Vikhlinin *et al.*, *Chandra Cluster Cosmology Project III: Cosmological Parameter Constraints,* arXiv:0812.2720 [astro-ph].

[17] S. Weinberg, *The cosmological constant problem,* Rev. Mod. Phys. **61** (1989) 1;
S. Weinberg, *The cosmological constant problems,* arXiv:astro-ph/0005265.

[18] V.A. Rubakov, *Large and infinite extra dimensions,* Phys. Usp. **44** (2001) 871 [Usp. Fiz. Nauk **171** (2001) 913] [arXiv:hep-ph/0104152].